

1 **Post-collisional magmatism in the central East African Orogen: the**
2 **Maevarano Suite of north Madagascar**

3
4 K. M Goodenough^{1,#}, R. J. Thomas², B. De Waele^{2*}, R. M. Key¹, D.I. Schofield², W.
5 Bauer^{2**}, R. M. Tucker³, J-M. Rafahatelo⁴, M. Rabarimanana⁴, A.V. Ralison⁴ and T.
6 Randriamananjara⁴

7 ¹*British Geological Survey, Murchison House, Edinburgh, EH9 3LA, U.K*

8 ²*British Geological Survey, Keyworth, NG12 5GG U.K.*

9 ³*United States Geological Survey, Reston, Va,20192 USA*

10 ⁴*Projet de Gouvernance des Ressources Minières, Ampandrianomby, Antananarivo, Madagascar*

11 ** Present address : SRK Consulting, Perth, Western Australia*

12 *** Present address: Geologisches Institut, RWTH-Aachen, 52056 Aachen, Germany*

13 *#: Corresponding author, kmgo@bgs.ac.uk Tel: 0044 131 6500272*

14
15 **Abstract**

16 Late tectonic, post-collisional granite suites are a feature of many parts of the Late
17 Neoproterozoic to Cambrian East African Orogen (EAO), where they are generally
18 attributed to late extensional collapse of the orogen, accompanied by high heat flow and
19 asthenospheric uprise. The Maevarano Suite comprises voluminous plutons which were
20 emplaced in some of the tectonostratigraphic terranes of northern Madagascar, in the
21 central part of the EAO, following collision and assembly during a major orogeny at ca.
22 550 Ma. The suite comprises three main magmatic phases: a minor early phase of foliated
23 gabbros, quartz diorites, and granodiorites; a main phase of large batholiths of porphyritic
24 granitoids and charnockites; and a late phase of small-scale plutons and sheets of
25 monzonite, syenite, leucogranite and microgranite. The main phase intrusions tend to be
26 massive, but with variably foliated margins. New U-Pb SHRIMP zircon data show that
27 the whole suite was emplaced between ca. 537 and 522 Ma. Geochemically, all the rocks
28 of the suite are enriched in the LILE, especially K, and the LREE, but are relatively

29 depleted in Nb, Ta and the HREE. These characteristics are typical of post-collisional
30 granitoids in the EAO and many other orogenic belts. It is proposed that the Maevarano
31 Suite magmas were derived by melting of sub-continental lithospheric mantle that had
32 been enriched in the LILE during earlier subduction events. The melting occurred during
33 lithospheric delamination, which was associated with extensional collapse of the East
34 African Orogen.

35

36 **Keywords**

37 Madagascar; Maevarano Suite; post-collisional magmatism; East African Orogen

38

39 **1. Introduction**

40 The island of Madagascar comprises a collage of Precambrian basement terranes,
41 overlain by Phanerozoic sedimentary basins along the west coast. The Precambrian
42 terranes were juxtaposed during the Neoproterozoic to Cambrian (Pan-African) East
43 African and Malagasy orogenies (Collins and Pisarevsky, 2005). The East African
44 Orogen (EAO; Fig. 1) extends from Egypt in the north to Antarctica in the south (Stern,
45 1994; Meert, 2003; Jacobs and Thomas, 2004) and represents the collision zone between
46 Neoproterozoic India, the Congo-Tanzania-Bangweulu block, and the Saharan
47 metacraton (Meert, 2003; Collins and Pisarevsky, 2005; Collins, 2006). Madagascar lies
48 in the heart of the EAO, and its basement rocks have been studied from a number of
49 viewpoints including metamorphic histories (e.g. Buchwaldt et al., 2003; Jöns et al.,
50 2006); structural geology (Collins et al., 2003a, b; Tucker et al., 2007; Thomas et al.,
51 2009) and magmatic processes (Nédélec et al., 1995; Paquette and Nédélec, 1998; Meert
52 et al., 2001). In this paper we focus on the post-collisional intrusions of the Maevarano
53 Suite of northern Madagascar, in order to understand the lithospheric processes related to
54 the latter stages of this major orogenic event. Our work is the result of a major World
55 Bank sponsored project, which involved re-mapping and sampling the basement rocks of
56 northern Madagascar, undertaken by a consortium of the British Geological Survey
57 (BGS), the United States Geological Survey (USGS), and GLW Conseil (GLW). The

58 results were presented in the form of geological maps of various scales and an
59 unpublished explanation (BGS-USGS-GLW, 2008).

60 Voluminous post-collisional granitoids are a major feature of the EAO (Black and
61 Liégeois, 1993; Küster and Harms, 1998; Meert, 2003; Jacobs et al., 2008). They are
62 typically alkaline and metaluminous in composition, and can be broadly characterised as
63 A-type granitoids under the classification of Whalen et al. (1987). In the southern part of
64 the EAO, in East Antarctica and Mozambique, peak metamorphism associated with
65 collision-induced crustal thickening occurred at ca. 555 Ma (Bingen et al., 2009) and
66 post-collisional magmas were emplaced between ca. 530 and 485 Ma, with a pulse of
67 voluminous granitoid and charnockite magmatism at 510 – 500 Ma (Jacobs et al., 2008).
68 In central Madagascar, alkaline granite sheets (termed ‘stratoid granites’) have been dated
69 at ca. 630 Ma (Nédélec et al., 1995; Paquette and Nédélec, 1998) and were considered to
70 be post-collisional, following a high-grade metamorphic episode at ca. 650 Ma (Meert et
71 al., 2003). In northern and central Madagascar, prograde metamorphism occurred
72 between 570 and 520 Ma (Jöns et al., 2006; Tucker et al., 2007), and a number of post-
73 collisional plutons were emplaced during the period 550 – 520 Ma (Tucker et al., 1999;
74 Kröner et al., 1999, 2000; Meert et al., 2001; Buchwaldt et al., 2003). In the northern part
75 of the EAO, many post-collisional potassic granitoids were emplaced, following crustal
76 thickening, between 630 and 470 Ma (Küster and Harms, 1998 (Sudan, Ethiopia and
77 Somalia); Be’eri-Shlevin et al., 2009a (Israel and Egypt)). However, it seems that
78 granitoids of this type are less abundant in the central EAO, in Mozambique north of the
79 Lurio Belt (Jacobs et al., 2008) and in Tanzania, where high-grade metamorphism is also
80 recorded between 655 and 520 Ma (Möller et al., 2000; Johnson et al., 2005). The cause
81 of this localisation of post-collisional granitoids in certain areas of the EAO remains
82 uncertain, although Jacobs et al. (2008) have suggested that it may be related to partial
83 lithospheric delamination in specific areas of the orogen. However, it is notable that post-
84 collisional granitoids in the EAO are commonly associated both spatially and temporally
85 with major shear zones; examples of such magmatic events occurred in the ca. 550 Ma
86 Angavo shear zone of central Madagascar (Grégoire et al., 2009), after ca. 530 Ma in the
87 Lurio Belt of Mozambique (Bingen et al., 2009) and at 570 – 520 Ma in the Palghat-
88 Cauvery shear zone of southern India (Santosh et al., 2005).

89

90

91 **2. Geology of northern Madagascar**

92 The Precambrian basement of northern Madagascar consists of four main tectonic
93 units (Collins and Windley, 2002; Collins, 2006, Thomas et al., 2009). The oldest of
94 these is the *Antongil Craton*, on the north-east coast (Fig. 2), which comprises Archaean
95 orthogneisses formed at ca. 3200 Ma and intruded by granitoids at ca. 2500 Ma (Tucker
96 et al., 1999; Paquette et al., 2003). The craton was intruded by a Palaeoproterozoic mafic
97 suite, but was apparently unaffected by Neoproterozoic magmatism (BGS-USGS-GLW,
98 2008).

99 Dominating most of central Madagascar, the *Antananarivo Craton* (Fig. 2),
100 comprises Neoproterozoic orthogneisses and supracrustal rocks (2520 - 2500 Ma; Tucker et
101 al., 1999; Kröner et al., 2000), including the *Tsaratanana Sheets*, which are generally
102 considered to be allochthonous (Collins et al., 2003a). The Antananarivo Craton is
103 tectonically overlain in the west by Proterozoic metasedimentary rocks of the Itremo and
104 Ikalamavony groups (Cox et al., 1998; Collins, 2006). The gneisses of the Antananarivo
105 Craton and the overlying metasedimentary rocks were intruded at 820 – 720 Ma by
106 extensive granitoid plutons (Handke et al., 1999; Tucker et al., 1999; Kröner et al., 2000),
107 and evidence for earlier magmatism at ca. 1000 Ma has recently been reported (Tucker et
108 al., 2007). The northern part of the Antananarivo Craton was intruded by ‘stratoid
109 granites’ at ca. 630 Ma (Nédélec et al., 1995; Paquette and Nédélec, 1998). High-grade
110 metamorphism, due to crustal thickening, occurred between 570 and 520 Ma (Kröner et
111 al., 2000; de Wit et al., 2001; Tucker et al., 2007; Grégoire et al., 2009) and post-
112 collisional granites were emplaced during the period 550 – 530 Ma (Tucker et al., 1999;
113 Kröner et al., 1999, 2000; Meert et al., 2001).

114 In the northernmost part of the island, the *Bemarivo Belt* (Fig. 2) comprises two
115 distinct Proterozoic metamorphosed volcano-sedimentary sequences intruded by
116 Neoproterozoic arc-related plutons (Thomas et al., 2009). The southern part of the belt
117 consists of a sequence of high-grade metasedimentary rocks (Sahantaha Group), which
118 were derived from a Palaeoproterozoic source, and were intruded at 750 Ma by an

119 extensive suite of plutonic rocks (Thomas et al., 2009). The northern part comprises two
120 ca. 750 – 720 Ma metamorphosed volcano-sedimentary sequences, the high-grade
121 Milanoa Group and lower-grade Daraina Group. These supracrustal rocks are also
122 intruded by plutonic rocks, which date from between 718 and 705 Ma (Thomas et al.,
123 2009). The components of the Bemarivo Belt are considered to have formed in an arc
124 setting, and were metamorphosed to varying grades during collision with cratonic
125 Madagascar at 560-530 Ma (Jöns et al, 2006; Thomas et al., 2009). They were
126 subsequently intruded by post-collisional granitoids, and one pluton from this suite has
127 previously been dated at ca. 520 Ma (Buchwaldt et al., 2003; Jöns et al., 2006).

128 The ‘suture zone’ between the Antananarivo and Antongil cratons, comprising
129 paragneisses with numerous units of mafic and ultramafic rock, has been termed the
130 ‘Betsimisaraka Suture Zone’ (Kröner et al., 2000; Collins and Windley, 2002). Our
131 mapping (BGS-USGS-GLW, 2008) has defined a broadly equivalent terrane, the
132 *Anaboriana-Manampotsy Belt*, which largely lies between the Bemarivo Belt and
133 Antananarivo Craton (Fig. 2), and extends southwards roughly along the eastern side of
134 the Antananarivo Craton. This terrane consists of Neoproterozoic metasedimentary rocks
135 that underwent metamorphism and extensive migmatization at the time of collision of the
136 Bemarivo Belt and Antananarivo Craton (BGS-USGS-GLW, 2008), and are intruded by
137 abundant post-collisional granitoids. On its northern margin, the Anaboriana-
138 Manampotsy Belt is separated from the Bemarivo Belt by a steep shear zone, the
139 Sandrakota Shear Zone. To the south, the Anaboriana-Manampotsy Belt appears to pass
140 into the major Angavo Shear Zone of Nédélec et al. (2000).

141 Between 2005 and 2008 the BGS-USGS-GLW consortium undertook a regional
142 geological survey of northern Madagascar, along with a regional stream sediment
143 sampling programme and representative rock sampling for whole-rock geochemistry and
144 U-Pb zircon geochronology. As part of this work, the voluminous post-collisional
145 intrusions that occur within the northern part of the Antananarivo Craton, the Bemarivo
146 Belt and, most especially, the intervening Anaboriana-Manampotsy Belt, were mapped
147 and termed the ‘*Maevarano Suite*’ after the river of that name, where the various phases
148 of the suite are superbly exposed (Fig. 2, 3). Previous workers had identified many of the
149 plutons, but had not distinguished them from the foliated, Neoproterozoic and older

150 intrusions which are also exposed in the area (e.g. Besairie, 1971; Hottin, 1972). Post-
151 collisional granitoids in the Bemarivo Belt were identified by Buchwaldt et al. (2003) in
152 the Marojejy region, but their full extent and volume has only now been recognised. The
153 geology, petrography, geochemistry, age and petrogenesis of the Maevarano Suite
154 plutons are the subject of this paper.

155 The components of the Maevarano Suite were identified under a range of names
156 by previous surveys. Most of the Maevarano Suite plutons were shown as “granites et
157 migmatites granitoïdes” and “charnockites” on the compilations of Besairie (1964, 1971),
158 but these also included arc-related plutonic rocks (mainly orthogneisses) in the Bemarivo
159 Belt that are now known to be older, between ca. 750 and 710 Ma (Thomas et al., 2009).
160 The 1: 2 million-scale tectonic compilation of Hottin (1972) showed the post-collisional
161 granitoids in the recently defined Anaboriana-Manampotsy Belt to be older than similar
162 intrusions in the Bemarivo Belt, which were indicated merely as “granitoïdes
163 indifférenciés”. Our new geological maps are thus the first to show the true extent of this
164 widespread suite of post-collisional plutons (Fig. 2, 3; BGS-USGS-GLW, 2008).

165 Previous work on the post-collisional plutons in northernmost Madagascar has
166 been limited. Medium- to coarse-grained, weakly foliated “charnockite” plutons,
167 intruding the Bemarivo Belt in the Marojejy area (Fig. 2), gave a U-Pb (single zircon
168 TIMS analysis) emplacement date of 521 ± 4 Ma (Buchwaldt et al., 2003). U-Pb dating
169 (in situ electron microprobe analysis of monazite) allowed Jöns et al. (2006) to identify
170 two metamorphic stages for this area: collisional metamorphism between ca. 560 and 530
171 Ma, and peak metamorphic temperatures (possibly associated with the post-collisional
172 magmatism) between ca. 520 and 510 Ma.

173

174 **3. Field relationships of the Maevarano Suite**

175 The Maevarano Suite consists of numerous batholiths and plutons of varying size,
176 extending throughout the Bemarivo and Anaboriana-Manampotsy belts and the northern
177 part of the Antananarivo Craton (Fig. 2). The intrusions are most abundant in the
178 Anaboriana-Manampotsy Belt, where they form around 50% of the total outcrop area.
179 The porphyritic granite and charnockite that make up the greater volume of the suite

180 characteristically form high mountain savannah country, with large whaleback and
181 pavement outcrops (Fig. 4a). These rocks underlie parts of the high mountains (>2200 m)
182 of the Marojejy massif in north-east Madagascar, and the mountain massifs around
183 Sandra Kota, through which the Maevarano River has carved a deep gorge. Around
184 Sandra Kota, a single batholith is exposed over an area of some 15 000 km², and affords
185 excellent outcrops which constitute the “Type Area” of the suite (Fig. 3). Rocks of the
186 Maevarano Suite differ from the older intrusions in the area in that they are typically
187 weakly foliated to unfoliated, although a more intense foliation is typically developed at
188 pluton margins and within ductile shear zones (Fig 4b, c). The older intrusions of the
189 suite tend to be more pervasively foliated than the younger intrusions.

190 The plutons of the Maevarano Suite are chiefly granitic, including some
191 charnockitic (orthopyroxene-bearing) types, but range through granodiorites to
192 monzonites and syenites (generally quartz-bearing). Some minor mafic (dioritic to
193 gabbroic) intrusions, which have igneous textures, are intimately associated with the acid
194 rocks in the field (Fig. 4 e,f). The whole suite can be broadly divided into three magmatic
195 phases: an early phase of foliated intrusions, which are most commonly granodioritic; a
196 main phase of voluminous granitoid and charnockite plutons; and a late phase comprising
197 chiefly granites and monzogranites.

198 *3.1 Early phase*

199 The early phase of the Maevarano Suite includes both the most mafic and the
200 most pervasively deformed intrusions. For example, early biotite- and hornblende-bearing
201 granodioritic to monzodioritic orthogneisses form elongate intrusions that crop out in the
202 Maevarano River valley (Fig. 3). One such body has been dated for this study. The
203 Maevarano Suite also includes minor volumes of early mafic phases, including
204 homogeneous, medium- to coarse-grained, greenish-grey, foliated quartz-diorite, and
205 coarse- to medium-grained, dark-grey to blue-grey gabbro. The gabbros in particular are
206 typically associated with, and cut by, intrusions of porphyritic granite, often in complex
207 associations, with several cross-cutting phases (Fig. 4e, f). For this reason these mafic
208 intrusions are attributed to the early phase of the suite, but they have not been dated.

209 Small pyroxenite pods occur at a few locations, though their relationship to the rest of the
210 suite is uncertain.

211 *3.2 Main phase*

212 The most common lithology of the Maevarano Suite is very coarse-grained, fairly
213 homogeneous, pinkish, typically porphyritic, biotite ± hornblende granite, with subhedral
214 to euhedral, pink K-feldspar megacrysts up to 2.5 cm in size. These granites form some
215 of the largest intrusions in the Maevarano Suite, irregular in shape and of batholithic
216 proportions. Large bodies of orthopyroxene-bearing granite are commonly associated
217 with the porphyritic granites and have been mapped as charnockite (BGS-USGS-GLW,
218 2008). Typically, they are coarse- to very coarse-grained, locally potassium feldspar- or
219 plagioclase-phyric (phenocrysts up to 2 cm across), and fresh samples are characterised
220 by the classic dark green colouration and resinous lustre, together with the presence of
221 macroscopic orthopyroxene (Fig. 4d). Many of these charnockite bodies occur in
222 association with pink porphyritic granite, but contacts between the two are rarely
223 exposed. Medium- to coarse-grained, non-porphyritic granitoids are also relatively
224 common, and considered to be part of the main granite-charnockite phase.

225 The central parts of the main phase plutons are typically unfoliated or weakly
226 foliated, but a fabric defined by orientation of planar minerals commonly appears towards
227 pluton margins. Locally, the porphyritic granitoids have been transformed to strongly
228 flattened augen gneisses in ductile shear zones up to several hundreds of metres wide
229 (Fig. 3). In undeformed zones, a primary, igneous flow orientation of K-feldspar
230 phenocrysts has been locally observed.

231 Enclave-rich zones are common within the Maevarano Suite granitoids. The
232 enclaves either take the form of well-defined, discoidal, magmatic enclaves, or more
233 diffuse, partially digested and feldspathised mafic xenoliths stoped from the enclosing
234 country rock gneisses. In some areas, rafts up to hundreds of metres long of country rock
235 granite and gneiss occur within the granite, particularly close to its margins. Enclaves are
236 less commonly observed within the charnockites and, where seen, tend to have much
237 higher contents of mafic minerals than those within the granites.

238 *3.3 Late phase*

239 Within the Anaboriana-Manampotsy Belt, a number of later plutons intrude the
240 porphyritic granites of the main phase (Fig. 3). In the northern part of the belt, elliptical
241 monzogranite plutons up to 5 km across intrude the porphyritic granitoids, and one of
242 these has been dated during this study. These monzogranites are typically coarse-grained,
243 equigranular, weakly foliated (strongly foliated at the margins), grey to pinkish-grey, and
244 biotite- and amphibole-bearing. Syenite plutons are also reported from inaccessible
245 regions in the Bealanana area (BGS-USGS-GLW, 2008). Other intrusions belonging to
246 the late phase, which also intrude main phase plutons, include variably foliated
247 leucogranite sheets (Fig. 3), one of which has been dated in this study, and late, dyke-like
248 intrusions up to 2 km long of unfoliated microgranite. One of the most distinctive of the
249 late phase intrusions is the ring-like Tampoketsa massif in the southern part of the
250 Anaboriana-Manampotsy Belt. It forms a pronounced circular topographic feature that
251 attains an altitude of nearly 1400 m and appears to be a primary igneous feature, not due
252 to late domal folding. The Tampoketsa intrusion is extremely magnetic compared to the
253 surrounding rocks and forms a major positive aeromagnetic anomaly. Summit exposures
254 show the main lithology to be light grey-pink, fine- to medium-grained, biotite-
255 hornblende alkaline microgranite with a variably-developed foliation. It is included with
256 the Maevarano Suite on the basis of lithological, petrographical and fabric similarities,
257 but it has not been dated.

258 Late minor veins, sheets and irregular intrusions are not common but do occur
259 locally. They include pegmatitic and aplitic granite intrusions, which tend to occur in
260 small swarms, and larger bodies of fine- to medium-grained granite. These are considered
261 to represent the youngest part of the late phase of the Maevarano Suite.

262

263 **4. Petrography**

264 *4.1 Early phase*

265 The early phase intrusions are the most mafic parts of the Maevarano Suite,
266 ranging from granodiorites, monzonites and monzodiorites, to diorites and gabbros. All
267 are medium- to coarse-grained. In the granitoids, plagioclase (20-30%) dominates over
268 K-feldspar (up to 10%). Up to 25% quartz is present, and mafic minerals include biotite,

269 clinopyroxene and amphibole in varying amounts. Minerals are typically allotriomorphic
270 and show a strong preferred orientation.

271 Samples of gabbro consist of plagioclase (~30-40%), clinopyroxene (25-35%),
272 amphibole (10-20%), biotite (5-10%), and opaque minerals (up to 5%) along with
273 accessory titanite and apatite. Up to 5% quartz occurs in some samples. While the
274 hydrous minerals (amphibole and mica) are clearly of secondary origin, primary sub-
275 ophitic textures are locally preserved.

276 *4.2 Main phase*

277 Typical porphyritic granite samples are coarse-grained hypersolvus granites, with
278 microperthitic potassium feldspar phenocrysts up to 2.5 cm in size, though averaging 1.5
279 cm. Overgrowths of plagioclase on the potassium feldspar phenocrysts are present in a
280 few samples. The modal mineralogy comprises quartz (~20-30%), poikilitic K-feldspar
281 (microperthitic microcline, ~30-40%), plagioclase (~15-20%), greenish-brown amphibole
282 (~10%), brown biotite (5-10%), clinopyroxene relics (up to 5 %) and accessory opaque
283 mineral phases (up to 3%), apatite, zircon ± allanite, with epidote, chlorite and muscovite
284 as minor alteration products. Myrmekitic quartz-feldspar intergrowths are common.
285 Feldspars are generally fresh, showing only limited amounts of alteration, and textures
286 are most commonly granoblastic. The charnockitic phases have broadly similar
287 mineralogy to the porphyritic granites, but with 5-20% orthopyroxene. In most samples,
288 the orthopyroxene is highly altered, and largely replaced by amphibole.

289 *4.3 Late phase*

290 Late phase granitoids are predominantly medium-grained, with allotriomorphic
291 textures, and are commonly quite fresh, although feldspars are locally sericitised. K-
292 feldspar (microperthitic microcline, ~ 25-40%) predominates over plagioclase (10-20%)
293 with up to 30% quartz. Mafic minerals are amphibole and biotite, with similar accessories
294 to the granitoids of the main phase.

295

296 **5. Geochronology**

297 Four samples belonging to the Maevarano Suite were selected for U-Pb zircon
298 geochronology. All the samples are from plutons emplaced into the Anaboriana-
299 Manampotsy Belt, where the Maevarano Suite intrusions are at their most voluminous.
300 Location information for the samples is given as grid references using the Laborde grid,
301 and localities are shown on Figs. 2 and 3. The zircon data are given in electronic
302 supplemental data tables A-D. The samples were chosen from older and younger phases,
303 on the basis of field relations, in order to bracket the emplacement age of the entire suite.
304 The charnockite phase from the Marojejy area in the Bemarivo Belt has been dated at 521
305 ± 4 Ma (Buchwaldt et al., 2003), so was not reinvestigated in this study. Three of our
306 samples were taken from the Maevarano River valley, where the field relationships
307 between the phases are clear. From this region we collected samples of: the early phase
308 (foliated quartz monzodiorite), which occurs as raft-like bodies in the porphyritic granite;
309 a foliated late phase leucogranite sheet cutting the porphyritic granite; and a late phase
310 monzonite pluton which intrudes both leuco- and porphyritic granite. The fourth sample
311 was collected from further south, where late veins and irregular bodies of granite cut
312 migmatitic gneisses of the Anaboriana-Manampotsy Belt.

313 *5.1 Methodology*

314 Zircons were separated from large, fresh rock samples using standard crushing,
315 washing, heavy liquid separation (LST and MI liquids) and magnetic separation (Frantz
316 Isodynamic Separator) techniques, followed by hand-picking under a binocular
317 microscope. The grains were mounted in epoxy, and polished mid-section to expose their
318 centre. Mounts were imaged using transmitted and reflected optical microscopy as well as
319 by cathodoluminescence (CL) on a Scanning Electron Microscope.

320 The zircons were dated using the Sensitive High Resolution Ion Microprobe
321 (SHRIMP) at Curtin University of Technology, Perth, Western Australia. Methodologies
322 for SHRIMP analyses followed those described in De Waele and Pisarevsky (2008).
323 Common Pb correction was carried out, using measured ^{204}Pb , and applying a common
324 Pb composition appropriate for the age of the zircon, following Stacey and Kramers
325 (1975). All pooled ages are reported at 95% confidence levels, while single data are
326 reported at 1 σ confidence level. SHRIMP data were reduced using the Squid plug-in for

327 Excel (Ludwig, 2001a), and plotted and interpreted using the Isoplot plug-in for Excel
328 (Ludwig, 2001b). All data are plotted uncorrected for non-radiogenic Pb.

329 5.2 Sample BT/07/12 [grid ref. 617845 1280192]

330 Sample BT/07/12 is a foliated quartz monzodiorite of the early phase, taken from
331 large river outcrops and pavements in the Maevarano River near Ambodirafia (Fig. 3).
332 The sampled lithology is medium- to coarse-grained, fresh, grey, hornblende-biotite
333 quartz monzodiorite, with a strong, sub-vertical foliation trending SSE-NNW. It is fairly
334 homogeneous, but locally has a weak layering defined by variations in grain size and
335 mineralogy, and most notably by layers with more or less K-feldspar. The rocks are
336 weakly migmatitic, with <5% layer-parallel leucocratic veins. These foliated quartz
337 monzodiorites to granodiorites occur as large enclaves, up to several hundreds of metres
338 wide, surrounded and veined by very coarse-grained, pink, porphyritic granite of the main
339 phase of the Maevarano Suite.

340 Zircons from sample BT/07/12 range in size from 50 to 200 μm and have length
341 to width ratios between 1:1 and 3:1. The crystals are rounded to subrounded and appear
342 colourless to pale pink in transmitted light. Most zircons contain some cracks, but have
343 only very small amounts of inclusions. CL images reveal dark CL-response, and faint
344 parallel zoning patterns (Fig. 5a-b). Some zircons appear to be overgrown by large high-
345 response domains that show no zoning. Large invasive zones of homogenisation,
346 recognised in many zircons, are interpreted to record solid-state recrystallisation.

347 16 analyses were conducted on this sample and indicate low f_{206} values up to
348 1.14% (Table A). U and Th are in the range 71-379 and 91-495 ppm respectively, with
349 the exception of analysis 6 (1196 and 2066 ppm). Th/U ratios are between 0.29 and 2.82,
350 extending well beyond the typical ratios expected for magmatic zircon ($0.5 < \text{Th}/\text{U} < 1.0$),
351 possibly due to some Th/U fractionation during solid-state recrystallisation.

352 Apart from three data points that record the highest common lead (Pb_c) values, the
353 data on cores define a concordant cluster (Fig. 6). The seven most concordant analyses
354 yield a concordia age of 531 ± 5 Ma (MSWD of concordance = 2.0). The relatively high
355 MSWD of concordance indicates some scatter in the dataset, but the age represents the
356 best estimate for crystallisation of zircon cores in sample BT/07/12. Six analyses

357 conducted on unzoned high-CL rims, although discordant due to incorrect correction for
358 Pb_c , seem to record slightly younger crystallisation ages around ~520 Ma. Although this
359 age cannot be fully resolved based on the data obtained, it does suggest crystallisation of
360 these rims immediately after the emplacement of the granite, perhaps from late-stage
361 fluids associated with the intrusion of the main phase granites.

362 *5.3 Sample BT/07/22 [grid ref. 610788 1269827]*

363 Sample BT/07/22 is from a small elliptical, late phase pluton near the Maevarano
364 River, where tor-like outcrops are characterised by a curious “fluted”, pot-holed
365 appearance. This pluton intrudes the main, porphyritic phase of the Maevarano Suite, and
366 is foliated within a few tens of metres of its margins, but elsewhere essentially unfoliated.
367 The sample is a homogeneous, slightly foliated, pinkish-grey, medium- to coarse-grained,
368 biotite-amphibole monzogranite. Sparse K-feldspars, up to 8 mm in size, are largely
369 perthitic. The rock contains a few discrete, spherical microdiorite xenoliths which were
370 carefully excluded from the analysed sample.

371 Zircon grains range in size from 100 to 300 μm and have aspect ratios between
372 2:1 and 4:1 (Fig. 5c-d). The crystals are clear, colourless to pale pink, and are commonly
373 cracked. CL imaging indicates single sector zoning, with alternating dark- and light-CL
374 zones (Fig. 5c-d). Zoning patterns and the high aspect ratios of most crystals suggest a
375 magmatic origin.

376 16 analyses were conducted and give f_{206} values between 0 and 2.66 (Table B). U
377 and Th values are low, between 26-128 and 46-239 ppm respectively, leading to high
378 proportions of apparent Pb_c based on very low counts on ^{204}Pb . None of the analyses
379 recorded more than 1 count over 10 second intervals, similar to measurements on
380 background, and this is taken to indicate extremely low Pb_c . Uncorrected data plot on
381 concordia and define a concordia age of 522 ± 6 Ma (MSWD of concordance = 0.50, Fig.
382 6), which we take to reflect the emplacement age of the monzogranite. One younger
383 analysis could represent crystallisation of zircon at ca. 464 ± 10 Ma (analysis 8), but more
384 likely represents a zircon that lost Pb.

385 *5.4 Sample BT/07/25 [grid ref. 606786 1267524]*

386 Sample BT/07/25 is from a late phase intrusion of the Maevarano Suite which
387 largely comprises fine- to medium-grained, foliated, biotite-bearing microgranite, and
388 which intrudes the porphyritic granite. The foliation in rocks of this microgranite is
389 variable, but commonly quite strong, and defined by small variations in mineralogy and
390 grain size. A slightly coarser-grained quartz-feldspar facies forms discontinuous layers
391 and blebs, defining a weak, diffuse layering. No mafic enclaves, blebs or schlieren have
392 been observed – the rocks are typically homogeneous at the outcrop scale. The sample is
393 a light grey, medium- to fine-grained, pinkish microgranite with a weak foliation formed
394 by alignment of mafic aggregates.

395 Zircon crystals are between 100 and 250 μm in size, and have aspect ratios
396 between 2:1 and 5:1 (Fig. 5e-f). The crystals are sub- to euhedral in shape, and have well-
397 defined crystal terminations. The crystals are virtually free of inclusions and cracks, and
398 vary between colourless and pale pink. CL images show concentric and parallel zones
399 that suggest a magmatic origin (Fig. 5e-f). A small number of larger zircons appear to
400 have a homogenous inner dark-CL core, overgrown by a medium-CL homogenous rim.

401 15 analyses were conducted on 15 zoned crystals and indicated low contents of
402 Pb_c with f_{206} between 0 and 1.09%, corresponding to less than one count on ^{204}Pb every
403 ten seconds (Table C). U and Th contents are in the range 161-734 and 116-1936 ppm
404 respectively, giving Th/U ratios between 0.57 and 2.85.

405 The data plot in a broad cluster on concordia, and the nine most concordant points
406 (after correction for non-radiogenic Pb) correspond to a concordia age of 527 ± 5 Ma
407 (MSWD of concordance=0.005), which we take to represent the best age estimate for the
408 emplacement of the microgranite (Fig. 6). The data points that plot slightly away from
409 this concordant cluster correspond to analyses that either recorded higher counts on ^{204}Pb ,
410 or some noise resulting in background counts in excess of counts on ^{204}Pb (but always
411 less than 1 count every 10 seconds). One analysis (15) recorded a concordant $^{206}\text{Pb}/^{238}\text{U}$
412 age of 541 ± 8 Ma, and may represent a slightly older xenocrystic component in the
413 sample.

414 *5.5 Sample RK7248A [grid ref. 632500 1175988]*

415 Sample RK7248A was collected from a ridge within the Anaboriana-Manampotsy
416 Belt (Fig. 2), with numerous rock pavements of agmatitic gneiss with a blocky grey
417 gneiss palaeosome surrounded by granitic leucosome, and cut by discrete veins and
418 irregular bodies of granite. The analysed sample was taken from one of the late granite
419 bodies.

420 Zircon crystals range in size from 100 to 200 μm and have aspect ratios between
421 2:1 and 5:1. The crystals are sub- to euhedral with well-developed terminations,
422 colourless to pale pink, with very few inclusions and virtually no cracks. CL images
423 reveal broad parallel or concentric zoning patterns consistent with magmatic
424 crystallisation (Fig. 5g-h). Several zircon grains are overgrown by narrow high-CL
425 unzoned rims, possibly related to a thermal episode that led to neocrystallisation of low-U
426 rims.

427 21 analyses yielded f_{206} values between 0 and 0.96%. U and Th are in the ranges
428 104-495 ppm and 53-217 ppm respectively, giving Th/U ratios between 0.25 and 1.12,
429 largely within the range expected for magmatic zircon (Table D). The data define a broad
430 cluster around concordia with weighted mean $^{206}\text{Pb}/^{238}\text{U}$ age of 532 ± 6 Ma (MSWD=5.4)
431 (Fig. 6). The high MSWD value for this calculation indicates significant scatter of
432 $^{206}\text{Pb}/^{238}\text{U}$ ratios, interpreted to reflect some Pb-loss in the zircons. Using only concordant
433 data, a concordia age of 537 ± 5 Ma (MSWD=0.35) can be calculated, which is
434 interpreted as the best estimate for the age of crystallisation of zircon in the sample. High
435 CL rims and magmatically zoned core domains provide similar ages, and this may
436 indicate that emplacement of the granitic protolith took place during a thermal event that
437 induced migmatitisation and fluid mobility in the rock.

438 In summary, the four analysed samples show a narrow spread of emplacement
439 ages from 537 ± 5 to 522 ± 6 Ma. The younger end of this range is consistent with the
440 emplacement of the Marojejy charnockite in the southern Bemarivo Belt at 520.9 ± 4.2
441 Ma (Buchwaldt et al., 2003) and in keeping with the age ranges of metamorphism in the
442 same area (Jöns et al., 2006, 2009). Very few older, inherited zircons were found,
443 suggesting that these magmas did not undergo substantial crustal contamination.

444

445 6. Geochemistry

446 30 whole-rock samples from representative Maevarano Suite intrusions and
447 phases have been analysed for major, trace and rare earth elements. Fresh rock samples
448 selected for geochemistry were crushed and milled in agate at the DMG Laboratory of the
449 Ministry of Energy and Mines in Antananarivo, and analysed at ACTLABS, Canada (by
450 their Code 4 Lithoresearch package). Major oxides and some trace elements were
451 analysed by Li-metaborate / tetraborate fusion with an ICP analysis, and these sample
452 solutions were further diluted and spiked for ICP-MS analysis. The samples were run for
453 major oxides and selected trace elements on a combination simultaneous/sequential
454 Thermo Jarrell-Ash ENVIRO II ICP or a Spectro Cirros ICP, and for other trace elements
455 on a Perkin Elmer SCIEX ELAN 6000 or 6100 ICP-MS. The data are given in Table 1;
456 details of repeat analyses on standards are presented as supplemental data in Table E..

457 The majority of samples (20) are granitoid rocks, including porphyritic granites
458 and charnockites, of the main granite-charnockite phase of the Maevarano Suite. Just one
459 (dated) granitoid sample is from the early phase, and four samples are gabbros that are
460 also considered to belong to the early phase. Five samples are from the late phase, and
461 include the dated monzogranite and leucogranite, along with the Tampoketsa alkaline
462 granite.

463 The analysed samples show a wide range in SiO₂ content, from 45 to 78 wt%, the
464 gabbros having < 55 wt% SiO₂ (Fig. 7). The majority of samples are low in MgO (<3%)
465 and show a negative correlation with SiO₂ (Fig. 7a), although the early phase samples
466 (gabbros and foliated quartz monzodiorite) have notably higher MgO (> 3.0%) than
467 granitoid samples with similar SiO₂. As would be expected, Fe₂O₃ shows a strong
468 negative correlation with SiO₂ (Fig. 7b), with the highest Fe₂O₃ contents in the gabbros
469 (> 10%) although some charnockites are also Fe₂O₃-rich. All granitoid samples are high
470 in K₂O (>3.5%) whereas gabbro samples have K₂O < 3.5% (Fig. 7c), and there is no
471 apparent correlation between K₂O and SiO₂ (Fig. 7c); this suggests buffering by a K-
472 bearing phase such as amphibole, phlogopite or K-feldspar during evolution of the
473 magmas (Williams et al., 2004). K₂O/Na₂O is >1 in most samples, again with the
474 exception of the four gabbro samples which have K₂O/Na₂O < 1. In the Total Alkalis vs

475 Silica (TAS) plot (Fig. 7d), most of the samples are alkalic under the classification of
476 Miyashiro (1974). This plot is most appropriate for volcanic rocks, and only provides a
477 crude method of classifying plutonic rocks. However, it is notable that, despite high
478 modal contents of K-feldspar, very few Maevarano Suite samples actually have the bulk
479 composition of true granite; many fall in the broad syenite and syeno-diorite fields, which
480 also encompass monzonitic compositions. The analysed samples are largely
481 metaluminous (molar $A/CNK < 1$) (Fig. 8a), although the most SiO_2 rich samples are
482 weakly peraluminous, suggesting the possibility of some crustal contamination of these
483 magmas.

484 In magmatic suites, such as the Maevarano Suite, that do not appear to have
485 suffered extensive post-crystallisation alteration, it is common to attempt to discriminate
486 the tectonic setting of granitoids using discrimination diagrams such as those of Pearce et
487 al. (1984). Granitoid samples from the Maevarano Suite are plotted on the (Y+Nb) vs Rb
488 plot of Pearce et al. (1984) (Fig. 8b) and although most plot in the within-plate granite
489 field, there is an overlap into the volcanic arc and syn-collisional granite fields. This
490 spread across fields is common in post-collisional granites (Pearce, 1996) and the
491 Maevarano Suite shows the same spread as other post-collisional granitoids from the
492 EAO (e.g. Roland, 2004; Küster and Harms, 1998). On the Ga/Al vs. Zr plot of Whalen
493 et al. (1987) the Maevarano Suite granitoids plot in the field of A-type granites (Fig. 8c),
494 as do other EAO post-collisional granites (Roland, 2004; Küster and Harms, 1998). In the
495 A-type granite classification of Eby (1990, 1992) the Maevarano Suite granitoids spread
496 across the A_1 and A_2 fields (Fig. 8d). Post-collisional granitoids would normally be
497 expected to fall in the A_2 field, which indicates magmas that may have been derived by
498 re-melting of crust. In contrast, magmas in the A_1 field are more likely to have been
499 derived from mantle sources (Eby, 1992).

500 Samples from the early phase show many consistent trace element characteristics
501 (Fig. 9a). Most are relatively enriched in Ba, K, and the LREE, with negative Ta-Nb
502 anomalies and depletion in the HREE relative to the LREE (La_N/Yb_N typically > 10). One
503 analysed sample, KGM48, lacks a Nb-Ta anomaly and has a relatively flat slope from the
504 LREE to the HREE, and it is possible that this intrusion was derived a different source to
505 the other Maevarano Suite magmas. Sample 497-JM-07 shows positive Sr, Ti and Eu

506 anomalies, suggesting that its bulk composition has been modified by crystal
507 accumulation (plagioclase and ilmenite) and cannot be used to approximate a magmatic
508 composition.

509 The more evolved samples of the main granite-charnockite phase show higher
510 contents of some of the Large Ion Lithophile Elements (LILE) (especially Rb, Th and K)
511 than the mafic samples of the early phase (Fig. 9b), but have many similar characteristics
512 including negative Nb-Ta anomalies and fractionated REE patterns ($La_N/Yb_N > 10$).
513 Strong negative Sr and Ti anomalies (and in one case a weak Eu anomaly) in the main
514 phase samples indicate that plagioclase and a Ti-rich mineral such as titanite or ilmenite
515 were fractionated as the magmas evolved.

516 Samples from the late magmatic phases can be divided into two groups on the
517 basis of their trace element patterns (Fig. 9c). Monzogranites and leucogranites of the
518 Maevarano River area have similar trace element patterns to the main phase granites,
519 though strong Eu and Sr negative anomalies indicate that these magmas are highly
520 evolved. Two samples from the Tampoketsa granite have pronounced negative Nb-Ta
521 anomalies and very low contents of the HREE ($La_N/Yb_N > 80$). These differences may
522 indicate a different source for this unusual intrusion. Low contents of HREE commonly
523 indicate the presence of garnet in the source of the magmas, and so it is possible that the
524 parental magma of the Tampoketsa granite was derived from greater depth than those of
525 other parts of the Maevarano Suite.

526 The similarity in geochemistry between most phases of the Maevarano Suite
527 supports the assignation of these intrusions to a single magmatic suite. These intrusions
528 show many of the typical features that have been recognised in post-collisional granitoids
529 of the EAO (Küster and Harms, 1998; Nédelec et al., 1995; Roland, 2004), including:
530 high contents of the LILE, especially K; negative Nb-Ta anomalies; and enrichment of
531 the LREE over the HREE. Perhaps the single most distinctive feature of these and other
532 post-collisional granitoids is that they plot in the A-type granite fields on discrimination
533 diagrams, yet have strong negative Nb-Ta anomalies which would not be expected in
534 granitoids formed in an intracontinental rift setting (Whalen et al., 1987).

535

536 **7. Discussion**

537 The Maevarano Suite of northern Madagascar comprises three recognisable
538 phases of intrusion, of which the second, main phase was the most voluminous. Both
539 field and geochronological evidence show that the suite was emplaced shortly after the
540 main deformation associated with the Malagasy orogeny – the last orogenic event to
541 affect the East African Orogen in Madagascar (Collins and Pisarevsky, 2005; Collins,
542 2006). In the field, some exposures show that the intrusive rocks, particularly of the late
543 phase, cut the main foliation in their country rocks. However, the contacts of granitoids of
544 the main phase are commonly broadly parallel to the regional fabrics and the granites are
545 themselves foliated at pluton margins, but unfoliated in their cores. Components of the
546 early phase tend to be pervasively foliated and form elongate bodies that are parallel to
547 the foliation in the host rocks. This indicates that the Maevarano Suite magmatism largely
548 post-dated the main crustal thickening event, but that the early phase intrusions were
549 emplaced during its waning stages.

550 In its type area, the Maevarano Suite is associated with a number of ductile shear
551 zones. This is a common association for post-collisional granites in the EAO, and in some
552 areas the later deformation on the shear zones has been associated with orogenic collapse
553 (Jacobs and Thomas, 2004; Jacobs et al., 2008; Bingen et al., 2009; Grégoire et al., 2009;
554 Viola et al., 2008). Although field evidence for this is limited in northern Madagascar, we
555 can use these analogies to tentatively suggest that the earliest Maevarano Suite magmas
556 were emplaced at the end of the collisional event, but that voluminous main phase
557 magmatism was associated with extensional collapse of the orogen, with extensional
558 shear zones providing the pathways for magma ascent.

559 The observed field relationships are consistent with the geochronology; high-
560 grade metamorphism in north Madagascar peaked at ca. 560 – 530 Ma (Jöns et al., 2006,
561 2009), and our work has shown that the earlier, foliated phases of the Maevarano Suite
562 were emplaced at ca. 537 – 531 Ma, with magmatism continuing until 520 Ma. A similar
563 pattern is recognised in central Madagascar, where metamorphism on the Angavo Shear
564 Zone occurred at ca. 550 Ma (Grégoire et al., 2009) followed by magmatism at ca. 550 –
565 530 Ma (Tucker et al., 1999; Kröner et al., 1999, 2000; Meert et al., 2001).

566 Petrography and geochemical analyses demonstrate that the Maevarano Suite
567 intrusions share many features - such as LILE enrichment, negative Nb-Ta anomalies,
568 and LREE enrichment over the HREE - with other post-collisional granitoids along the
569 length of the EAO. A number of apparent contradictions characterise these post-
570 collisional granitoids: for instance, charnockites typically indicate water-undersaturated
571 magmas, yet they are associated with amphibole-bearing granites that are likely to have
572 formed from hydrous magmas. Similarly, discrimination diagrams indicate that these are
573 A-type granites, yet they have the strong Nb-Ta negative anomaly commonly found in
574 arc settings. Such Nb-Ta anomalies could be partly caused by contamination with local
575 crustal material, but it is notable that the anomalies are present even in the most mafic
576 magmas that are likely to be relatively uncontaminated. The lack of older xenocrystic
577 zircons in the dated samples also provides an argument against substantial crustal
578 contamination of the magmas.

579 The consistency of many main geochemical features of post-collisional intrusions
580 along the EAO suggests the likelihood of a common source for the majority of these
581 magmas. The granitoids are largely metaluminous, rather than peraluminous, indicating
582 that they were not generated solely by the melting of local crustal material, although the
583 more silica-rich magmas are likely to have been affected by some crustal contamination.
584 Recent studies have proposed that the source of post-collisional magmas elsewhere in the
585 EAO was in the mafic lower crust (e.g. Jacobs et al., 2008); but the lower crust is likely
586 to be depleted in the LILE rather than enriched (Pearce, 1996), and so does not represent
587 a feasible source for the K-rich Maevarano Suite. A growing consensus (e.g. Pearce,
588 1996; Liégeois et al., 1998; Bonin, 2004) is that the source for K-rich post-collisional
589 magmas is in the sub-continental lithospheric mantle (SCLM), which has been
590 heterogeneously enriched through metasomatism by LILE-enriched fluids derived by
591 dehydration of a subducting slab. Such slab fluids are typically characterised by low Nb-
592 Ta contents (Fitton, 1995) and thus the enriched SCLM would also have low amounts of
593 these elements. Partial melting of such a source could produce the LILE-enriched, Nb-
594 Ta- poor magmas of the Maevarano Suite, and we suggest that other post-collisional
595 magmas in the EAO were also derived from metasomatised SCLM. In northern
596 Madagascar, there is abundant evidence for subduction during the Neoproterozoic, prior

597 to collision of the terranes that make up the island (e.g., arc-like magmas; Thomas et al.,
598 2009), and enrichment of the SCLM could have occurred at this time. In the north of the
599 EAO, alkaline parts of the post-collisional granitoid suite have similarly been attributed
600 to a lithospheric mantle source that was metasomatised during Neoproterozoic subduction
601 (Be'eri-Shlevin et al., 2009b).

602 The transition from crustal shortening to extension in many orogenic belts,
603 including the EAO, has been explained in terms of delamination of part, or all, of the sub-
604 continental lithospheric mantle (Houseman and Mackenzie, 1981; Black and Liégeois,
605 1993; Jacobs et al., 2008). Such delamination allows hot asthenospheric material to well
606 up, heating the upper part of the lithospheric mantle and promoting melting (Schott and
607 Schmeling, 1998). Bonin (2004) proposed a model for collisional to post-collisional
608 magmatism that commences with lithospheric stacking, producing peraluminous magmas
609 derived by melting of continental crust which mingle with small-degree potassic melts
610 from the SCLM. This is followed by slab break-off and lithospheric delamination,
611 removing part of the lithospheric mantle keel and melting the upper part of the SCLM to
612 produce medium- to high-K magmas. Finally, this model (Bonin, 2004) suggests that
613 over a period of millions of years the SCLM thickens by cooling and underplating of
614 deeper material, and alkaline magmas of within-plate type are derived from deeper levels.
615 The majority of the Maevarano Suite magmas can be related to the slab break-off/
616 lithospheric delamination stage of this model. However, the youngest Tampoketsa granite
617 may have been formed by melting of deeper SCLM and could represent the evolution to a
618 true within-plate setting; it is possible that it is rather younger than the rest of the
619 Maevarano Suite.

620 Within northern Madagascar, the Maevarano Suite intrusions are abundant within
621 some crustal units (the Anaboriana-Manampotsy and Bemarivo belts, and parts of the
622 Antananarivo Craton) but are absent in others (the Antongil Craton). Two explanations
623 can be postulated: 1) a suitable source was not present beneath the Antongil Craton; 2)
624 structural controls led to the emplacement of magmas only in certain areas.

625 Evidence to support the first explanation comes from study of the Neoproterozoic
626 history of the terranes of northern Madagascar. The Bemarivo Belt and the Antananarivo

627 Craton both contain abundant Neoproterozoic subduction-related magmatic suites (820-
628 700 Ma; Handke et al., 1999; Tucker et al., 1999; Kröner et al., 2000; Thomas et al.,
629 2009), which provide evidence for a subduction event prior to collision that could have
630 enriched the SCLM. The country rocks of the Anaboriana-Manampotsy Belt are entirely
631 Neoproterozoic (BGS-USGS-GLW, 2008) and may represent an arc sequence preserved
632 within the suture zone between continental fragments. In contrast, there is no evidence of
633 Neoproterozoic magmatism within the Antongil Craton (BGS-USGS-GLW, 2008). We
634 therefore postulate that the SCLM beneath the Antongil Craton was not enriched by
635 subduction-related fluids prior to continental collision, and thus was less hydrous and
636 more viscous than the SCLM beneath other parts of northern Madagascar. This unaltered
637 lithospheric mantle may simply not have delaminated (e.g. Elkins-Tanton, 2005), or may
638 have lacked fusible material that could be melted to produce post-collisional magmas.

639 Evidence for the second explanation comes from the common association of
640 Maevarano Suite granitoids with major shear zones, which seem to be focused
641 particularly along terrane boundaries. As suggested above, the Antongil Craton may have
642 had a thicker, more viscous lithospheric root than the surrounding mobile belts, and so
643 may have behaved in a rigid fashion, leading to the development of shear zones along the
644 craton margins during collapse of the orogen (cf. Black and Liégeois, 1993). Magmas
645 were then emplaced along these shear zones.

646 It is likely that both these possible explanations are valid, and indeed linked.
647 Areas which had undergone Neoproterozoic subduction had hydrous, relatively dense
648 metasomatised SCLM that was a candidate both for delamination and for partial melting.
649 In contrast, areas that were unaffected by Neoproterozoic subduction were relatively
650 rigid, with anhydrous lithospheric roots that were not highly susceptible to either
651 delamination or melting. Shear zones, which developed at the boundaries between these
652 two types of terranes, focused the post-collisional magmas.

653

654 **8. Conclusions**

655 The Maevarano Suite of northern Madagascar consists largely of granitoid
656 intrusions, with minor early mafic phases, which were emplaced between ca. 537 and 522

657 Ma during the waning stages of the East African Orogen. Plutons of the Maevarano Suite
658 are commonly associated with ductile shear zones, which may have developed during
659 extensional collapse of the orogen. Distinctive geochemical features of these intrusions,
660 including LILE enrichment, negative Nb-Ta anomalies, and LREE enrichment over
661 HREE, point to a source in metasomatised sub-continental lithospheric mantle.
662 Maevarano Suite plutons are situated in areas where there is evidence for Neoproterozoic
663 subduction, but absent from areas that were not reworked at that time. We therefore
664 propose that the SCLM was metasomatised during Neoproterozoic subduction events and
665 subsequently melted during lithospheric delamination; areas such as the Antongil Craton
666 whose SCLM was not metasomatised, either did not delaminate, or were less susceptible
667 to partial melting. The magmas were then emplaced along crustal-scale shear zones.

668 Many of the conclusions drawn from this work can be applied along the length of
669 the EAO, where similar post-collisional plutons are common. We suggest that the source
670 for most of these post-collisional magmas is likely to lie in the SCLM, and that abundant
671 post-collisional plutons will be focused in areas where that SCLM was metasomatised
672 through Proterozoic subduction.

673

674 **Acknowledgments**

675 The authors would like to thank the many BGS, USGS and Malagasy colleagues who
676 were involved in fieldwork in Madagascar during 2005-2007. Martin Gillespie is thanked
677 for constructive comments on an earlier version, and Alan Collins and Joachim Jacobs
678 are thanked for their detailed and thoughtful reviews, all of which greatly improved the
679 manuscript. Editorial comments by Nelson Eby were also much appreciated. This paper
680 is published with the permission of the Executive Director of the British Geological
681 Survey (NERC). Age data in this paper were obtained at the Perth Consortium SHRIMP
682 facilities at the Curtin University of Technology, which are funded by the Australian
683 Research Council.

684

685 **References**

686 Be'eri-Shlevin, Y., Katzir, Y., Whitehouse, M., 2009a. Post-collisional tectonomagmatic
687 evolution in the northern Arabian-Nubian Shield: time constraints from ion-probe
688 U-Pb dating of zircon. *Journal of the Geological Society of London* 166, 71-85.

689 Be'eri-Shlevin, Y., Katzir, Y., Valley, J.W., 2009b. Crustal evolution and recycling in a
690 juvenile continent: Oxygen isotope ratio of zircon in the northern Arabian-Nubian
691 Shield. *Lithos* 107, 169-184

692 Besairie, H., 1964. Madagascar carte géologique. Service Géologique à Madagascar,
693 Tananarive.

694 Besairie, H., 1971. Carte Géologique à 1/2000000 et notice explicative, No. 189. Bureau
695 de Géologie Madagascar, Tananarive.

696 BGS-USGS-GLW, 2008. Revision de la cartographie géologique et minière des zones
697 Nord et Centre de Madagascar, République de Madagascar Ministère de
698 L'Energie et des Mines, Antananarivo.

699 Bingen, B., Jacobs, J., Viola, G., Henderson, I. H. C., Skar, Ø., Boyd, R., Thomas, R.J.,
700 Solli, A., Key, R.M., Daudi, E.X.F., 2009. Geochronology of the Precambrian
701 crust in the Mozambique belt in NE Mozambique, and implications for Gondwana
702 assembly. *Precambrian Research* 170, 231-255.

703 Black, R., Liégeois, J.P., 1993. Cratons, mobile belts, alkaline rocks and continental
704 lithospheric mantle; the Pan-African testimony. *Journal of the Geological Society*
705 *of London* 150, 89-98.

706 Bonin, B., 2004. Do coeval mafic and felsic magmas in post-collisional to within-plate
707 regimes necessarily imply two contrasting, mantle and crustal, sources? A review.
708 *Lithos* 78, 1-24.

709 Buchwaldt, R., Tucker, R.D., Dymek, R.F., 2003. Geothermobarometry and U-Pb
710 Geochronology of metapelitic granulites and pelitic migmatites from the Lokoho
711 region, Northern Madagascar. *American Mineralogist* 88, 1753-1768.

712 Collins, A.S., Windley, B.F., 2002. Tectonic evolution of central and northern
713 Madagascar and its place in the final assembly of Gondwana. *Journal of Geology*
714 110, 325-339.

715 Collins, A.S., Fitzsimons, I.C.W., Hulscher, B., Razakamanana, T., 2003a. Structure of
716 the eastern margin of the East African Orogen in central Madagascar.
717 *Precambrian Research* 123, 111-133.

718 Collins, A.S., Johnson, S., Fitzsimons, I.C.W., Powell, C.M., Hulscher, B., Abello, J. and
719 Razakamanana, T., 2003b. Neoproterozoic deformation in central Madagascar: a
720 structural section through part of the East African Orogen. In: Yoshida, M.,
721 Windley, B., and Dasgupta, S. (Eds.) *Proterozoic East Gondwana: Supercontinent*
722 *Assembly and Breakup*. Special Publication of the Geological Society, London
723 206, 363-379.

724 Collins, A.S., Pisarevsky, S.A., 2005. Amalgamating eastern Gondwana: The evolution
725 of the Circum-Indian Orogens. *Earth Science Reviews* 71, 229-270.

726 Collins, A.S., 2006. Madagascar and the amalgamation of Central Gondwana. *Gondwana*
727 *Research* 9, 3-16.

728 Cox, R., Armstrong, R.A., Ashwal, L.D., 1998. Sedimentology, geochronology and
729 provenance of the Proterozoic Itremo Group, central Madagascar, and
730 implications for pre- Gondwana palaeogeography. *Journal of the Geological*
731 *Society* 155, 1009-1024.

732 De Waele, B., Pisarevsky, S.A. 2008. Geochronology, paleomagnetism and magnetic
733 fabric of metamorphic rocks in the northeast Fraser Belt, Western Australia.
734 Australian Journal of Earth Sciences 55, 605-621.

735 De Wit, M.J., Bowring, S.A., Ashwal, L.D., Randrianasolo, L.G., Morel, V.P.I.,
736 Rabeloson, R.A., 2001. Age and tectonic evolution of Neoproterozoic ductile
737 shear zones in southwestern Madagascar, with implications for Gondwana studies.
738 Tectonics 20, 1-45.

739 Eby, G.N., 1990. The A-type granitoids: A review of their occurrence and chemical
740 characteristics and speculations on their petrogenesis. Lithos 26, 115-134.

741 Eby, G.N., 1992. Chemical subdivision of the A-type granitoids: Petrogenetic and
742 tectonic implications. Geology 20, 641-644.

743 Elkins-Tanton, L.T., 2005. Continental magmatism caused by lithospheric delamination.
744 In: Foulger G.R., Natland J.H., Presnall D.C., Anderson D.L. (Eds.), Plates,
745 Plumes and Paradigms: Geological Society of America Special Paper 388, 449-
746 461.

747 Fitton, J.G., 1995. Coupled molybdenum and niobium depletion in continental basalts.
748 Earth and Planetary Science Letters 136, 715-721.

749 Gillespie, M.R., Styles, M.T., 1999. Rock Classification Scheme Volume 1,
750 Classification of Igneous Rocks. British Geological Survey, Keyworth,
751 Nottingham.

752 Gregoire, V., Nédélec, A., Monie, P., Montel, J-M., Ganne, J., Ralison, B., 2009.
753 Structural reworking and heat transfer related to the late Panafrican Angavo shear
754 zone of Madagascar. Tectonophysics 477, 197-216

755 Handke, M., Tucker, R.D., Ashwal, L.D., 1999. Neoproterozoic continental arc
756 magmatism in west-central Madagascar. Geology 27, 351-354.

757 Hottin, G., 1972. Madagascar: Représentation schématique du volcanisme, de la
758 tectonique cassante, et des formations précambriennes. Echelle 1:2,000,000
759 Bureau de Recherches Géologiques et Minières, Limoges, France.

760 Houseman, G.A., McKenzie, D.P., 1981. Convective instability of a thickened boundary
761 layer and its relevance for the thermal evolution of continental convergent belts.
762 Journal of Geophysical Research 86, 6115-6132.

763 Jacobs, J., Bingen, B., Thomas, R.J., Bauer, W., Wingate, M.T.D., Feitio, P., 2008. Early
764 Palaeozoic orogenic collapse and voluminous late-tectonic magmatism in
765 Dronning Maud Land and Mozambique: insights into the partially delaminated
766 orogenic root of the East African - Antarctic Orogen. In: Satish-Kumar, M.,
767 Motoyoshi, Y., Osanai, Y., Hiroi, Y. and Shiraishi, K. (Eds.) Geodynamic
768 Evolution of East Antarctica: A Key to the East–West Gondwana Connection.
769 Geological Society of London Special Publication 308, 69-90.

770 Jacobs, J. Thomas, R.J., 2004. Himalayan-type indenter-escape tectonics model for the
771 southern part of the late Neoproterozoic-early Palaeozoic East African-Antarctic
772 orogen. Geology 32, 721-724.

773 Johnson, S.P., Rivers, T., De Waele, B., 2005. A Review of the Mesoproterozoic to early
774 Palaeozoic magmatic and tectonothermal history of south-central Africa:
775 implications for Rodinia and Gondwana. Journal of the Geological Society of
776 London 162, 433-450.

777 Jöns, N., Emmel, B., Schenk, V., Razakamanana, T., 2009. From orogenesis to passive

778 margin—the cooling history of the Bemarivo Belt (N Madagascar), a multi-
779 thermochronometer approach. *Gondwana Research* 16, 72-81.

780 Jöns, N., Schenk, V., Appel, P., Razakamanana, T., 2006. Two-stage metamorphic
781 evolution of the Bemarivo Belt of northern Madagascar: constraints from reaction
782 textures and in situ monazite dating. *Journal of Metamorphic Geology* 2006(24),
783 10.

784 Kröner, A., Hegner, E., Collins, A.S., Windley, B.F., Brewer, T.S., Razakamanana, T.,
785 Pidgeon, R.T., 2000. Age and magmatic history of the Antananarivo Block,
786 central Madagascar, as derived from zircon geochronology and Nd isotopic
787 systematics. *American Journal of Science* 300(4), 251-288.

788 Kröner, A., Windley, B.F., Jaeckel, P., Brewer, T.S., Razakamanana, T., 1999. New
789 zircon ages and regional significance for the evolution of the Pan-African orogen
790 in Madagascar. *Journal of the Geological Society, London* 156, 1125-1135.

791 Küster, D., Harms, U., 1998. Post-collisional potassic granitoids from the southern and
792 northwestern parts of the Late Neoproterozoic East African Orogen: a review.
793 *Lithos* 45, 177-195.

794 Le Bas, M.J., Le Maitre, R.W., Streckeisen, A., Zanettin, B., 1986. A chemical
795 classification of volcanic rocks based on the total alkali-silica diagram. *Journal of*
796 *Petrology* 27, 745-750.

797 Liégeois, J.P., Navez, J., Hertogen, J., Black, R., 1998. Contrasting origin of post-
798 collisional high-K calc-alkaline and shoshonitic versus alkaline and peralkaline
799 granitoids. The use of sliding normalization. *Lithos* 45, 1-28.

800 Ludwig, K.R., 2001a. *Squid 1.02: A User's Manual*. 2, Berkeley Geochronology Center,
801 Berkeley.

802 Ludwig, K.R., 2001b. *Isoplot/Ex rev. 2.49*, Berkeley Geochronology Centre, Berkeley,
803 California.

804 McDonough, W.F., Sun, S.-s., 1995. The Composition of the Earth. *Chemical Geology*
805 120, 223-253.

806 Meert, J.G., 2003. A synopsis of events related to the assembly of eastern Gondwana.
807 *Tectonophysics* 362(1-4), 1-40.

808 Meert, J.G., Nédélec, A., Hall, C., 2003. The stratoid granites of central Madagascar:
809 paleomagnetism and further age constraints on Neoproterozoic deformation.
810 *Precambrian Research* 120, 101-129.

811 Meert, J.G., Nédélec, A., Hall, C., Wingate, M.T.D., Rakotondrazafy, M., 2001.
812 Paleomagnetism, geochronology and tectonic implications of the Cambrian-age
813 Carion Granite, central Madagascar. *Tectonophysics* 340, 1-21.

814 Miyashiro, A., 1974. Volcanic rock series in island arcs and active continental margins
815 *American Journal of Science* 274, 321-355.

816 Möller, A., K., M., Schenk, V., 2000. U-Pb dating of metamorphic minerals: Pan-African
817 metamorphism and prolonged slow cooling of high pressure granulites in
818 Tanzania, East Africa. *Precambrian Research* 104, 123-145.

819 Nédélec, A., Ralison, B., Bouchez, J.-L., Gregoire, V., 2000. Structure and
820 metamorphism of the granitic basement around Antananarivo: A key to the Pan-
821 African history of central Madagascar and its Gondwana connections. *Tectonics*
822 19, 997-1020.

823 Nédélec, A., Stephens, W.E., Fallick, A.E., 1995. The Panafrican stratoid granites of

824 Madagascar: alkaline magmatism in a post-collisional extensional setting. *Journal*
825 *of Petrology* 36, 1367-1391.

826 Norconsult Consortium, 2007. Mineral Resources Management Capacity Building
827 Project, Republic of Mozambique. Component 2: Geological Infrastructure
828 Development Project, Geological Mapping. Report of the National Directorate of
829 Geology, Republic of Mozambique.

830 Paquette, J.L., Moine, B., Rakotondrazafy, M.A.F., 2003. ID-TIMS using the step-wise
831 dissolution technique versus ion microprobe U-Pb dating of metamict Archean
832 zircons from NE Madagascar. *Precambrian Research* 121(1-2), 73-84.

833 Paquette, J.-L., Nédélec, A., 1998. A new insight into Pan-African tectonics in the East-
834 West Gondwana collision zone by U-Pb zircon dating of granites from central
835 Madagascar. *Earth and Planetary Science Letters* 155, 45-56.

836 Pearce, J.A., 1996. Sources and settings of granitic rocks. *Episodes* 19(4), 120-125.

837 Pearce, J.A., Harris, N.B.W., Tindle, A.G., 1984. Trace element discrimination diagrams
838 for the tectonic interpretation of granitic rocks. *Journal of Petrology* 25, 956-983.

839 Roland, N.W., 2004. Pan-African Granite-Charnockite Magmatism in Central Dronning
840 Maud Land, East Antarctica: Petrography, Geochemistry and Plate Tectonic
841 Implications. *Geol. Jb.* B96, 187-231.

842 Santosh, M., Tanaka, K., Yokoyama, K., Collins, A.S., 2005. Late Neoproterozoic-
843 Cambrian Felsic Magmatism Along Transcrustal Shear Zones in Southern India:
844 U-Pb Electron Microprobe Ages and Implications for the Amalgamation of the
845 Gondwana Supercontinent. *Gondwana Research* 8, 31-42.

846 Schott, B., Schmeling, H., 1998. Delamination and detachment of a lithospheric root.
847 *Tectonophysics* 296, 225-247.

848 Stacey, J.S., Kramers, J.D., 1975. Approximation of terrestrial lead isotopic evolution by
849 a two-stage model. *Earth and Planetary Science Letters* 26, 207-221.

850 Stern, R.J., 1994. Arc Assembly and continental collision in the Neoproterozoic East
851 African orogeny - implications for the consolidation of Gondwana. *Annual*
852 *Reviews of Earth and Planetary Sciences* 22, 319-351.

853 Thomas, R.J., De Waele, B., Schofield, D.I., Goodenough, K.M., Horstwood, M., Tucker,
854 R.D., Bauer, W., Annells, R., Howard, K., Walsh, G., Rabarimanana, M.,
855 Rafahatelo, J.-M., Ralison, A.V., Randriamananjara, T., 2009. Geological
856 evolution of the Neoproterozoic Bemarivo Belt, northern Madagascar.
857 *Precambrian Research* 172, 279-300.

858 Tucker, R.D., Ashwal, L.D., Handke, M.J., Hamilton, M.A., Le Grange, M., Rambeloson,
859 R.A., 1999. U-Pb geochronology and isotope geochemistry of the Archean and
860 proterozoic rocks of north-central Madagascar. *Journal of Geology* 107(2), 135-
861 153.

862 Tucker, R.D., Kusky, T.M., Buchwaldt, R., Handke, M.J., 2007. Neoproterozoic nappes
863 and superposed folding of the Itremo Group, west-central Madagascar *Gondwana*
864 *Research* 12, 356-379.

865 Viola, G., Henderson, I.H.C., Bingen, B., Thomas, R.J., Smethurst, M., De Azavedo, S.,
866 2008. Growth and collapse of a deeply eroded orogen: insights from structural and
867 geochronological constraints on the Pan-African evolution of NE Mozambique.
868 *Tectonics* 27, doi:10.1029/2008TC002284

869 Whalen, J.B., Currie, K.L., Chappell, B.W., 1987. A-type granites: geochemical

870 characteristics, discrimination and petrogenesis. Contributions to Mineralogy and
871 Petrology 95, 407-419.

872 Williams, H.M., Turner, S.P., Pearce, J.A., Kelley, S.P., Harris, N.B.W., 2004. Nature of
873 the Source Regions for Post-collisional, Potassic Magmatism in Southern and
874 Northern Tibet from Geochemical Variations and Inverse Trace Element
875 Modelling. Journal of Petrology 45, 555-607.

876

877

878 **Figure list for Maevarano Paper**

879

880 **Figure 1:** Reconstruction of the East African Orogen, showing the palaeoposition of
881 Madagascar in Gondwana, after Jacobs and Thomas (2004) and Thomas et al. (2009).

882

883 **Figure 2:** Simplified geological map of northern Madagascar, showing the outcrop
884 pattern of the Maevarano Suite. The inset shows the main geological units of the whole of
885 Madagascar. BE – Bemarivo Belt; AB – Anaboriana-Manampotsy Belt; AN – Antongil
886 Craton; NT – Antananarivo Craton; IT – South Madagascar domains, including Itremo
887 Group; VO – Vohibory Domain; NB- Northern Bemarivo terrane; SB – Southern
888 Bemarivo terrane. The site of one of the dated samples is shown (RK7248A); other
889 sample locations are shown on Fig. 3.

890

891 **Figure 3:** Geological map of the type area of the Maevarano Suite, in the Maevarano
892 River valley south of Sandra Kota, showing the localities of three of the dated samples.

893

894 **Figure 4:** a) Typical Maevarano Suite landscape, with high mountain and valley
895 outcrops; b) Typical unfoliated porphyritic granitoid of the main phase; c) Typical
896 foliated porphyritic granitoid from margin of main phase pluton; d) Pegmatitic facies of
897 main phase charnockite with dark-brown weathering orthopyroxenes and dark green
898 hornblende; e) Foliated layered gabbro of early phase of Maevarano Suite intruded by
899 coarse-grained pegmatite veins associated with the main phase; f) Foliated layered gabbro
900 of early phase cut by foliated felsic sheets, in turn intruded by main phase granitoid
901 (upper third of picture) with foliated margin.

902

903 **Figure 5:** CL images of zircons from the dated samples, showing some of the analysed
904 spots: a) and b) – zircons from BT/07/12; c) and d) – zircons from BT/07/22; e) and f) –
905 zircons from BT/07/25; g) and h) – zircons from RK7248A.

906

907 **Figure 6:** Tera Wasserburg data plots for the four dated samples. Error crosses at 2σ .
908 Data not corrected for common Pb.

909

910

911 **Figure 7:** a-c) Harker plots for Maevarano Suite samples; d) Total Alkali vs Silica plot
912 for Maevarano Suite samples. Classification fields from Gillespie and Styles (1999) after
913 Le Bas et al. (1986). Alkalic/sub-alkalic division from Miyashiro (1974)

914

915 **Figure 8:** a) Plot of A/CNK (molar $\text{Al}_2\text{O}_3/(\text{CaO} + \text{Na}_2\text{O} + \text{K}_2\text{O})$) vs A/NK (molar
916 $\text{Al}_2\text{O}_3/(\text{Na}_2\text{O} + \text{K}_2\text{O})$) for Maevarano Suite samples. b): (Y+Nb) vs Rb granite
917 discrimination plot for granitoid samples from the Maevarano Suite, after Pearce et al.
918 (1984). Dashed line indicates field of other post-collisional granitoids from the East
919 African Orogen, from the Northern EAO, Mozambique, and Antarctica; data from Küster
920 and Harms, 1998; Roland, 2004; Norconsult, 2007. c): Ga/Al vs Zr granite discrimination
921 plot for granitoid samples from the Maevarano Suite, after Whalen et al. (1985). Dashed
922 line indicates field of other post-collisional granitoids from the East African Orogen,
923 from Mozambique and Antarctica; data from Roland, 2004; Norconsult, 2007. d):
924 Granitoid samples from the Maevarano Suite plotted on the Y-Nb-Ce discrimination plot
925 for A-type granites of Eby (1992). Dashed line indicates approximate field of other post-
926 collisional granitoids from the East African Orogen, from the Northern EAO,
927 Mozambique, and Antarctica; data from Küster and Harms, 1998; Roland, 2004;
928 Norconsult, 2007.

929

930 **Figure 9:** Primitive mantle-normalised trace element patterns for selected samples from
931 the early phase (a), main phase (b) and late phase (c) of the Maevarano Suite.
932 Normalising factors from McDonough and Sun (1995).

933

934

935 **Table 1:** Whole-rock major, trace and rare earth element data for all analysed samples.

936

937 Supplemental data tables

938

939 **Table A:** Geochronological data table for Sample BT/07/12

940

941 **Table B:** Geochronological data table for Sample BT/07/22

942

943 **Table C:** Geochronological data table for Sample BT/07/25

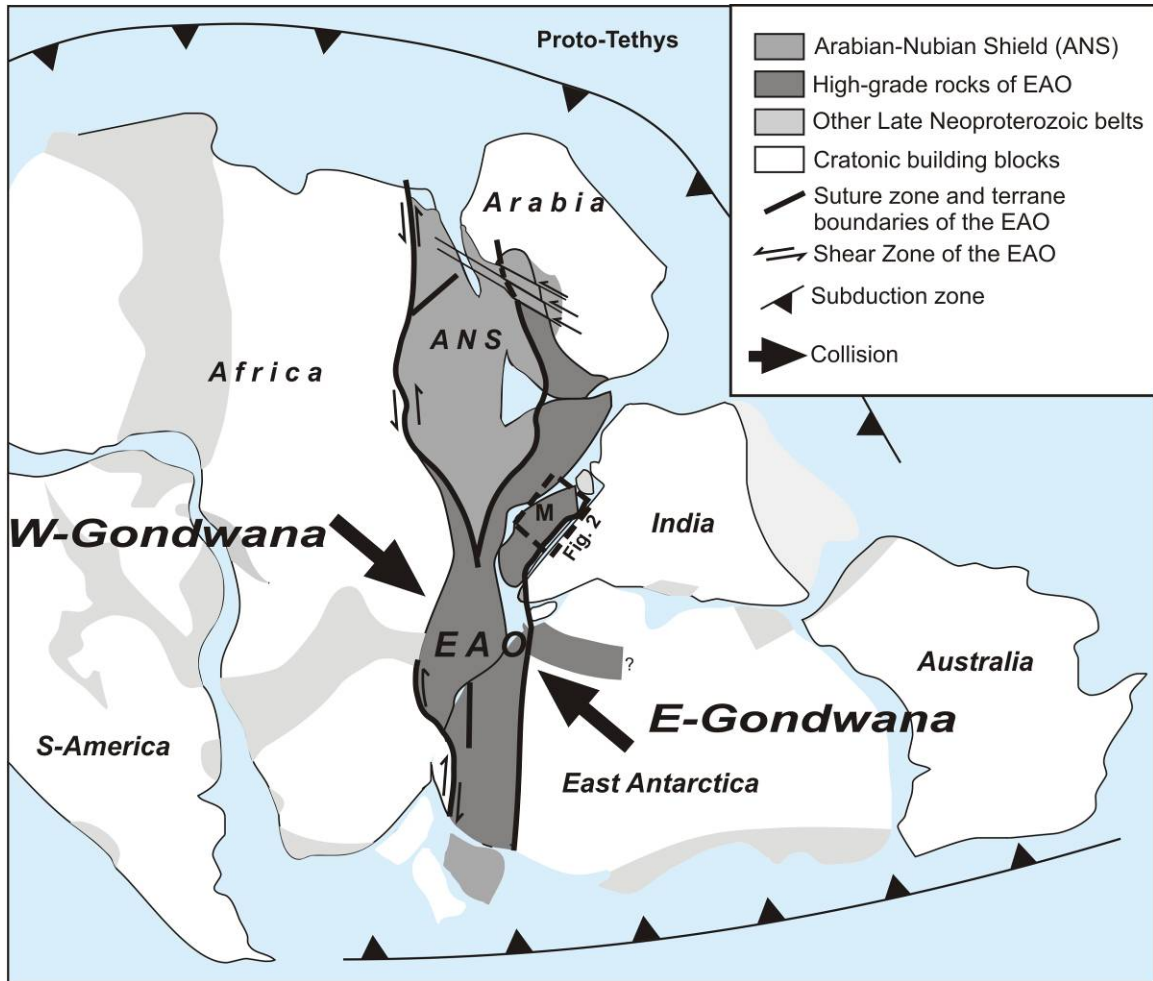
944

945 **Table D:** Geochronological data table for Sample RK7248A

946

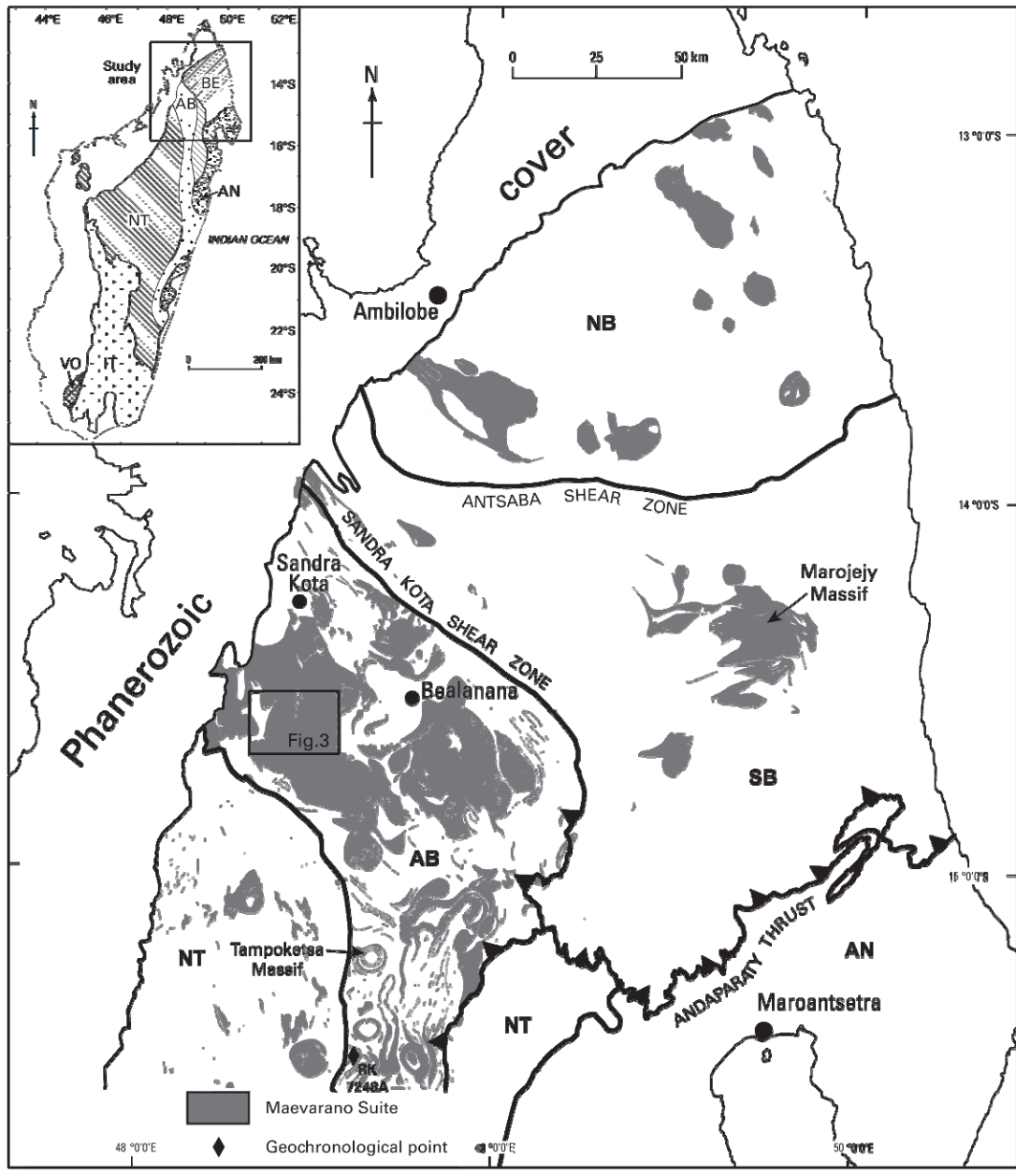
947 **Table E:** Measured and certificated results for standards, measured with two analytical
948 batches in which the samples described in this paper were run.

949



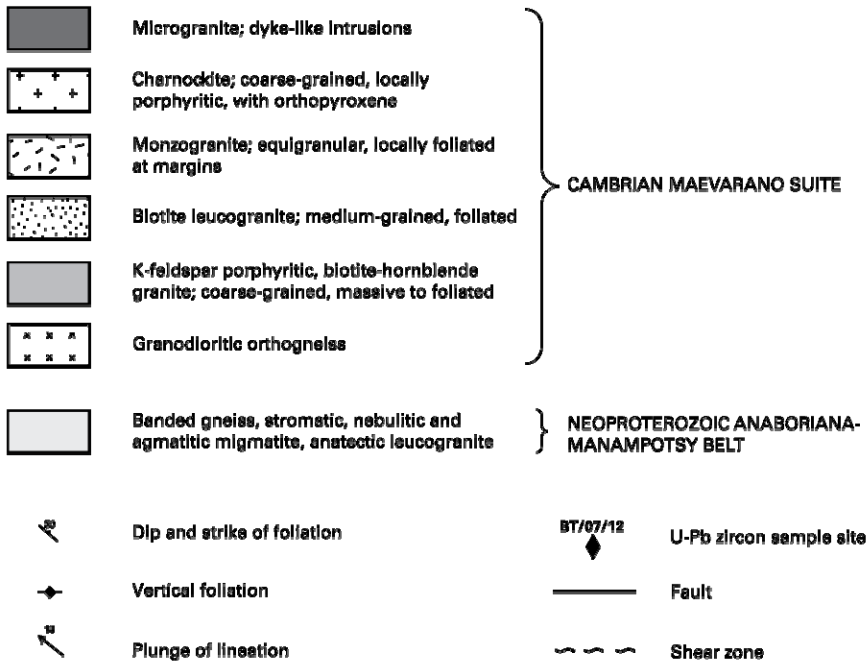
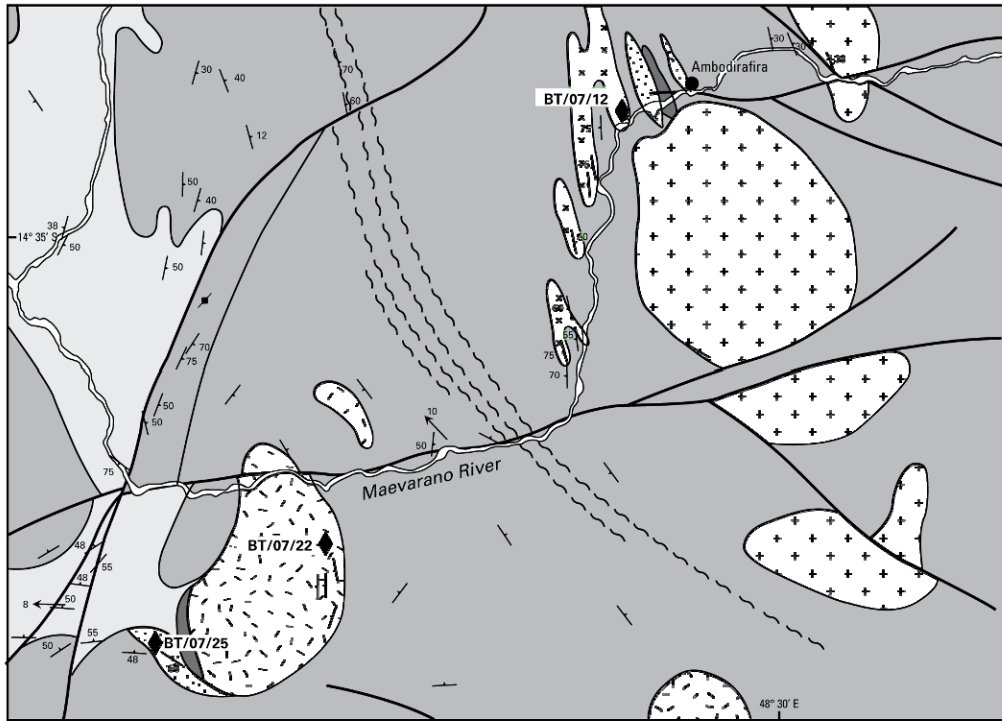
950

951 Fig. 1



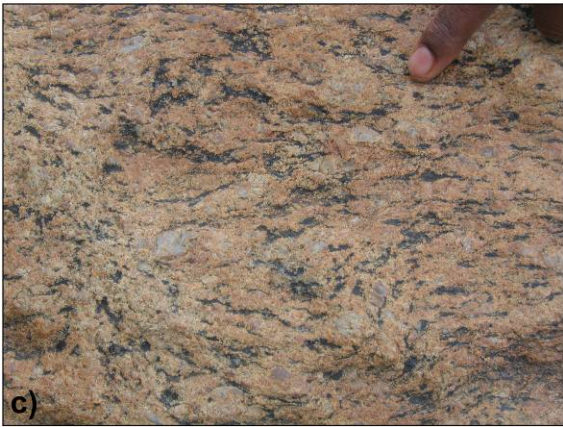
952

953 Fig 2



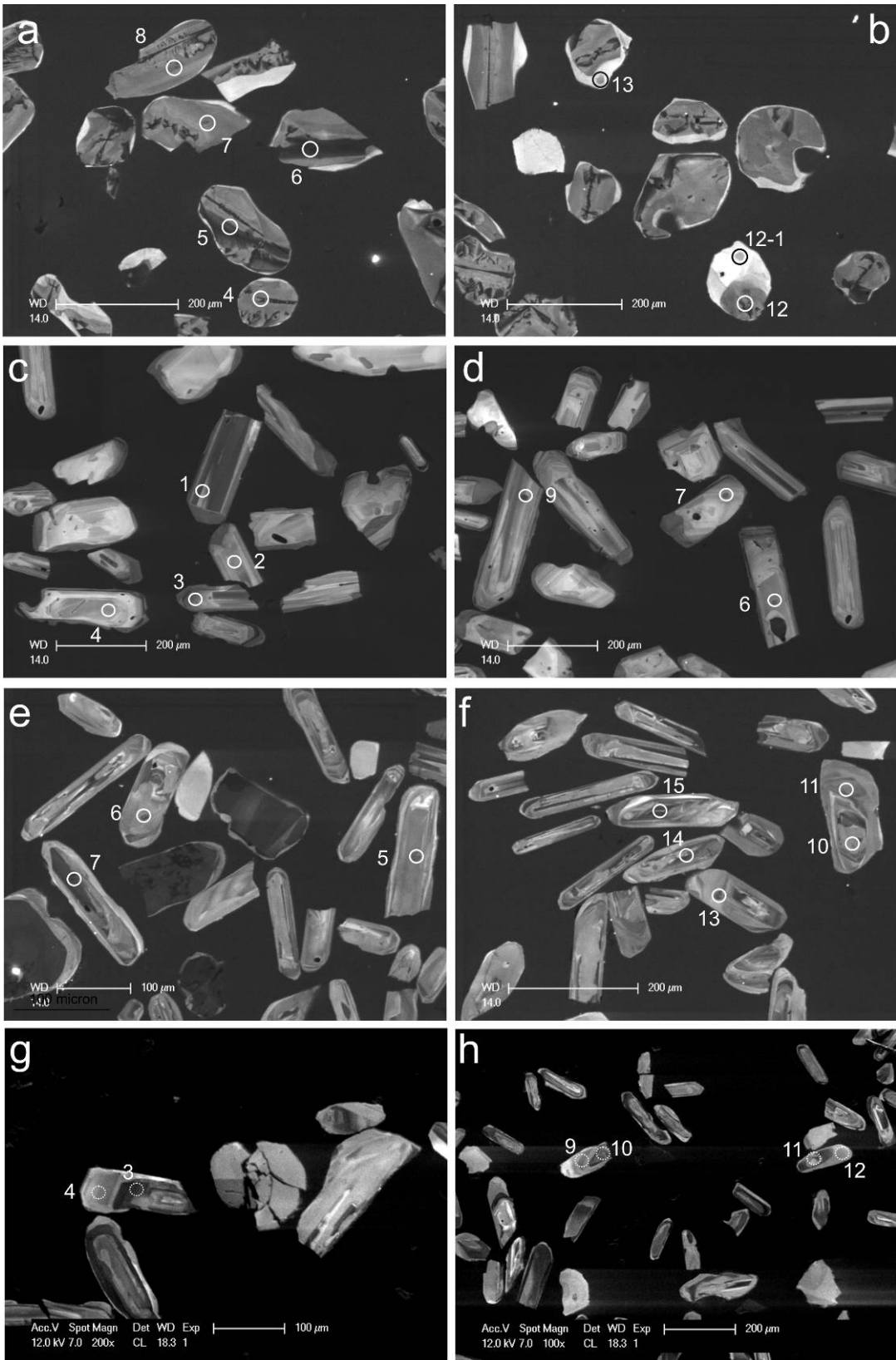
954

955 Fig 3



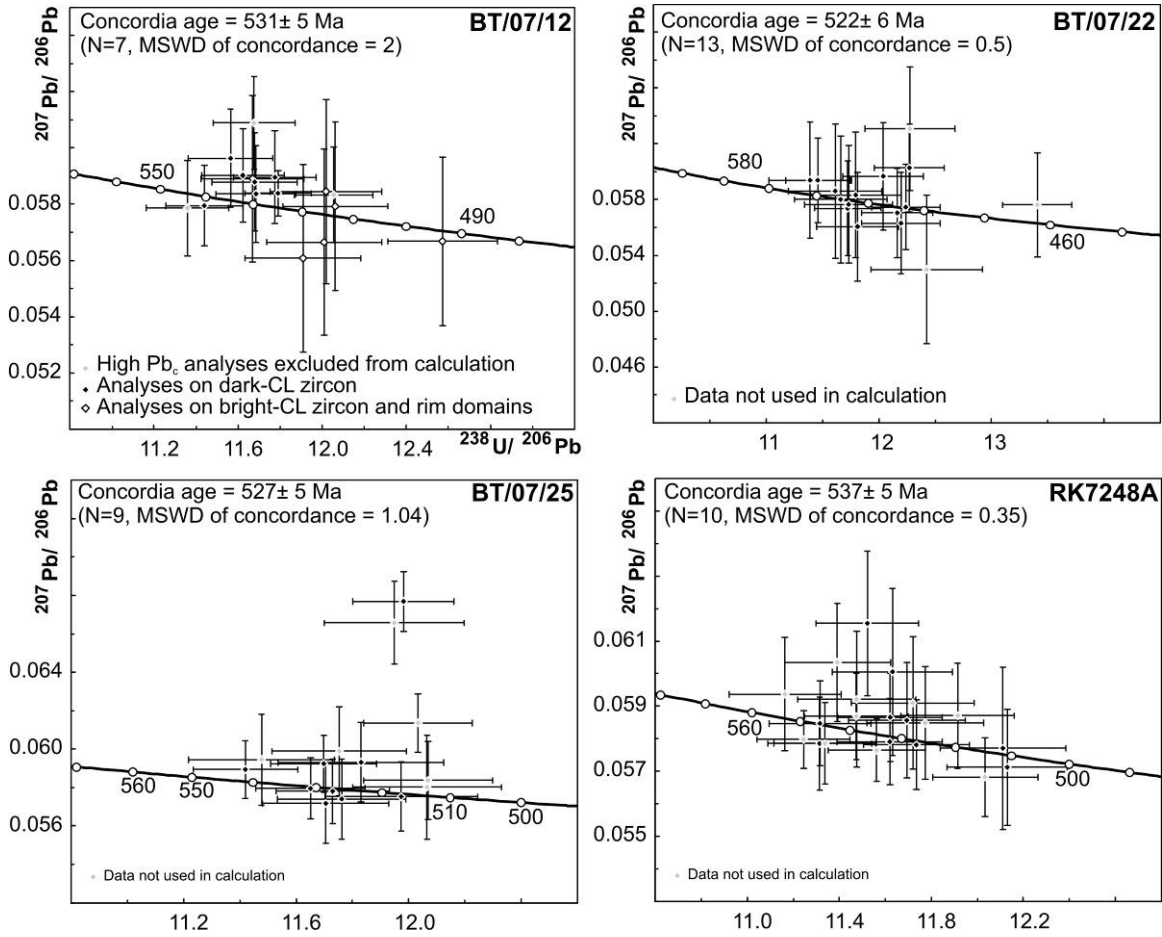
956

957 Fig 4



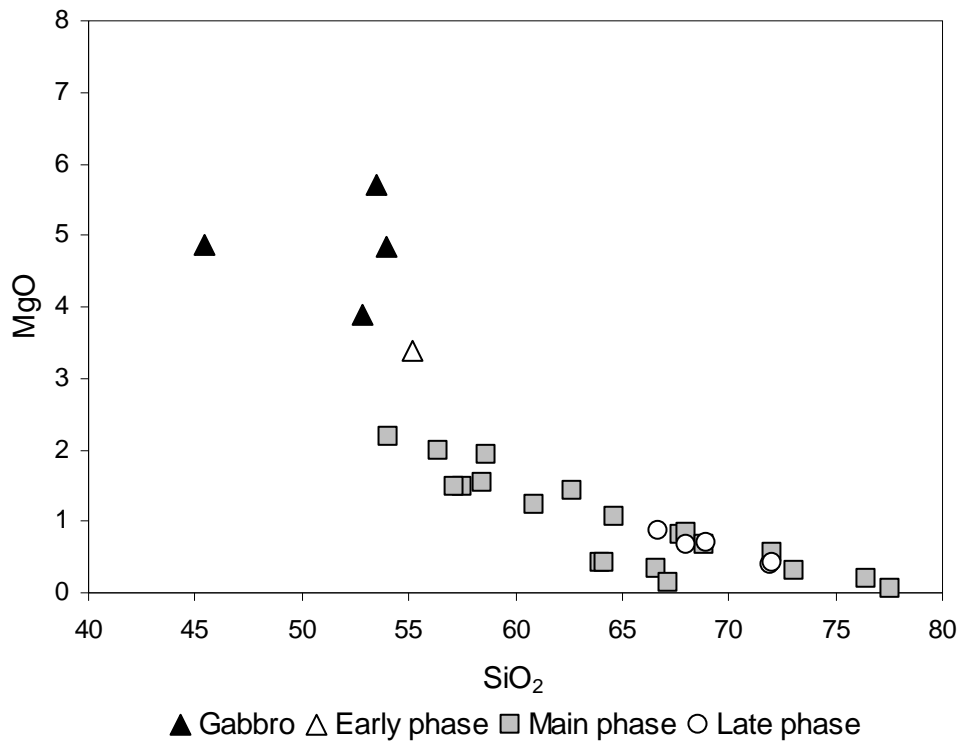
958

959 Fig 5

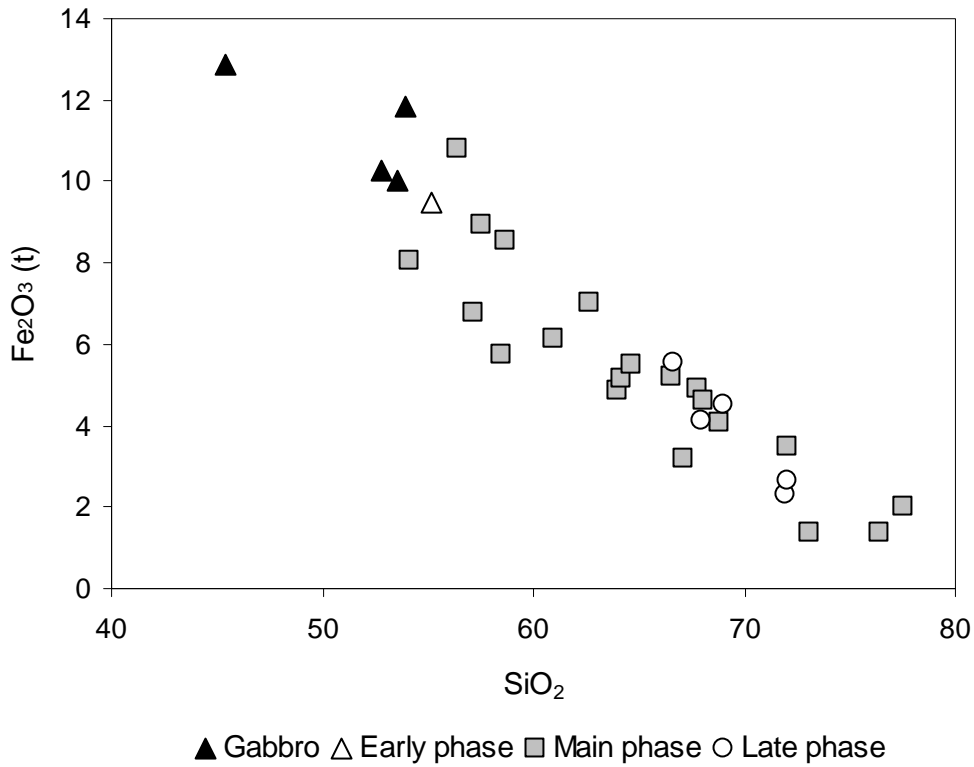


960

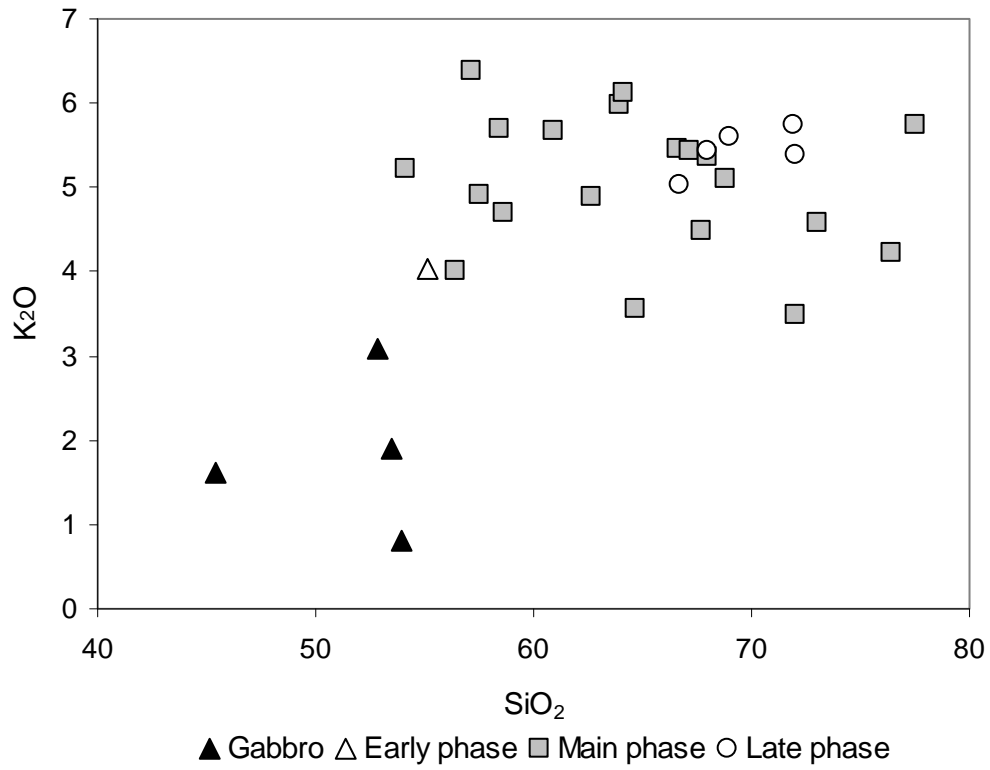
961 Fig 6



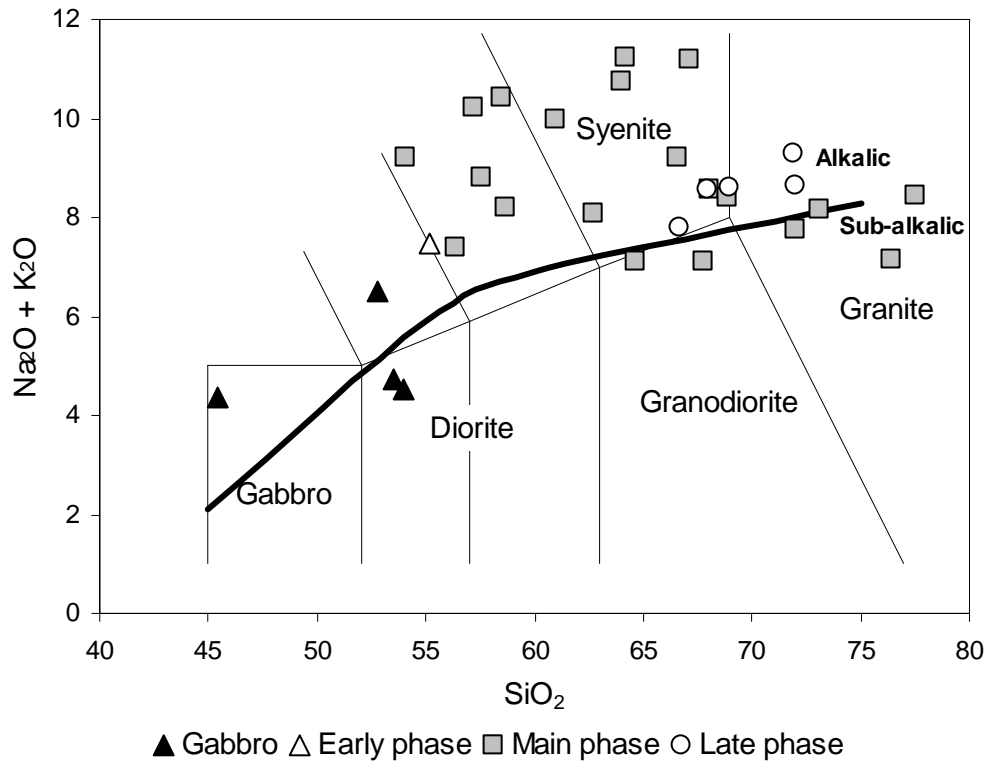
962 Fig. 7 a)
963



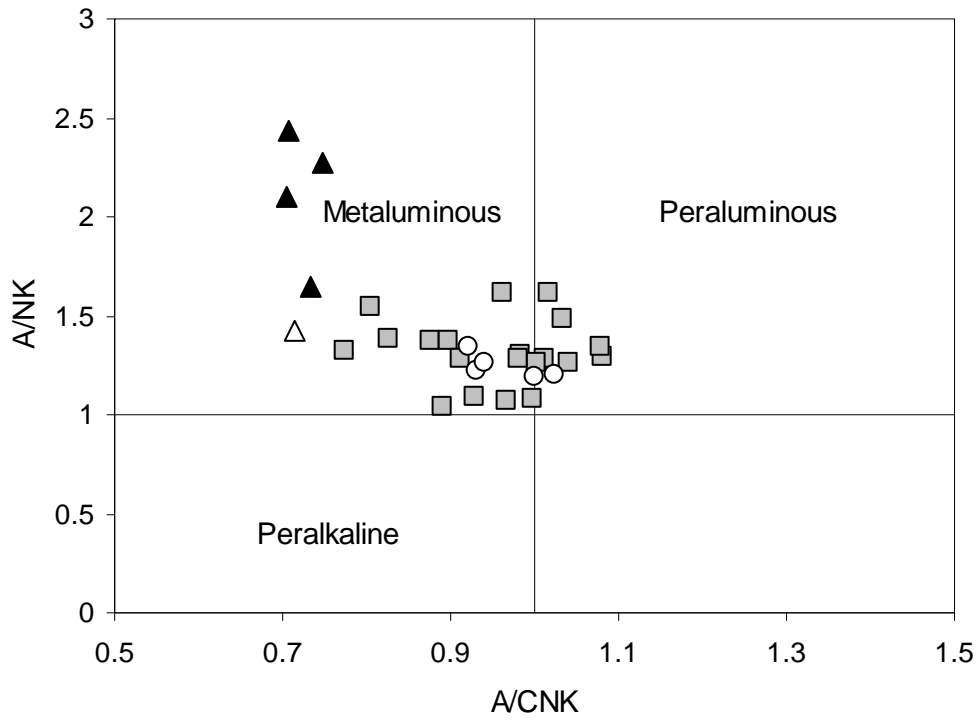
964 Fig. 7 b)
965
966



967
968 Fig. 7 c)

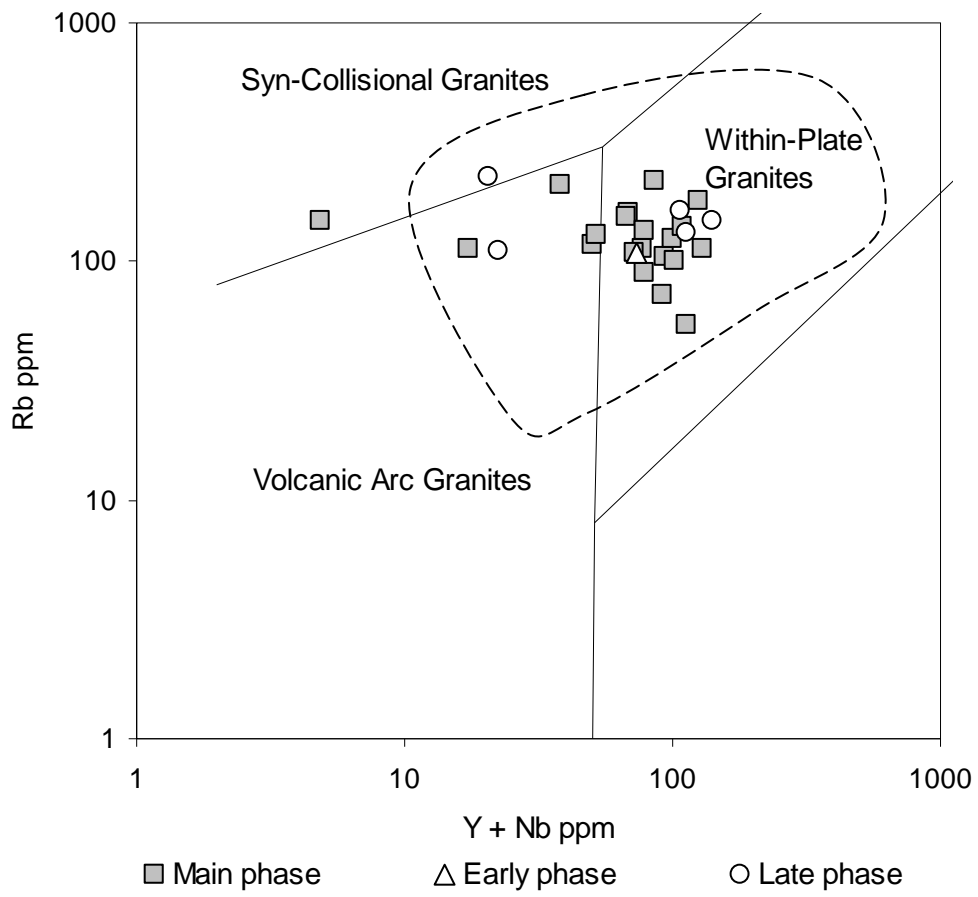


969
970 Fig. 7 d)

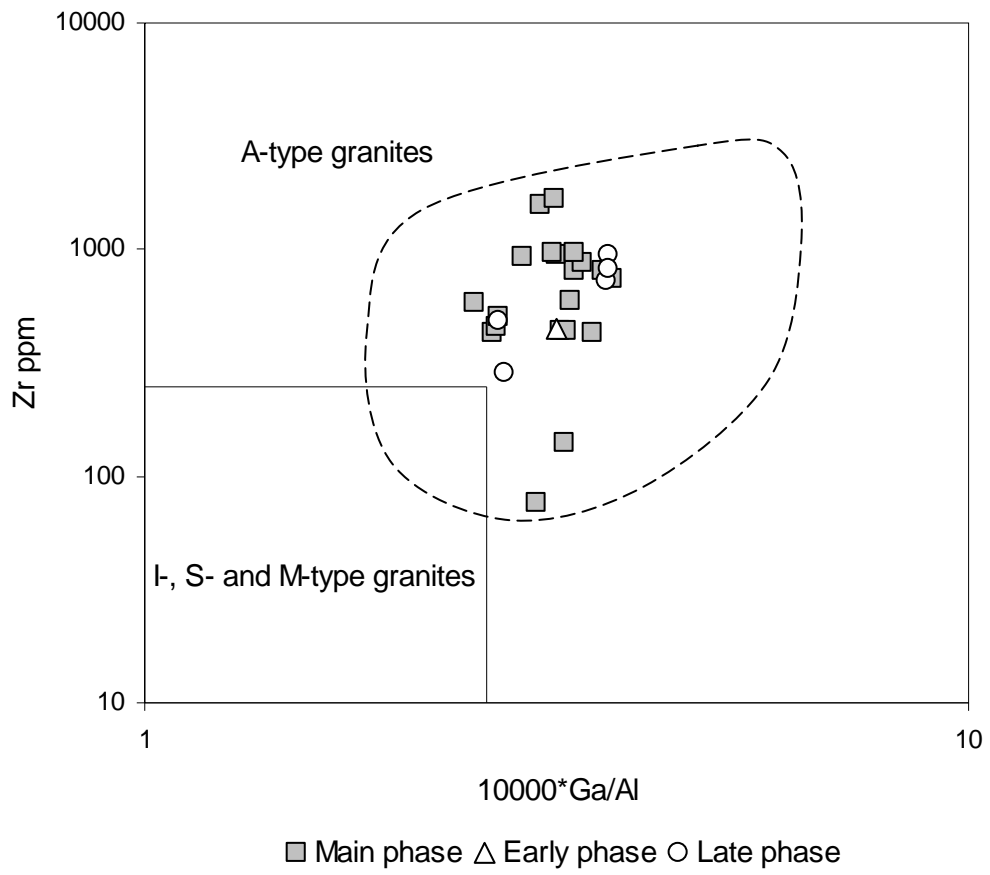


▲ Gabbro △ Early phase ■ Main phase ○ Late phase

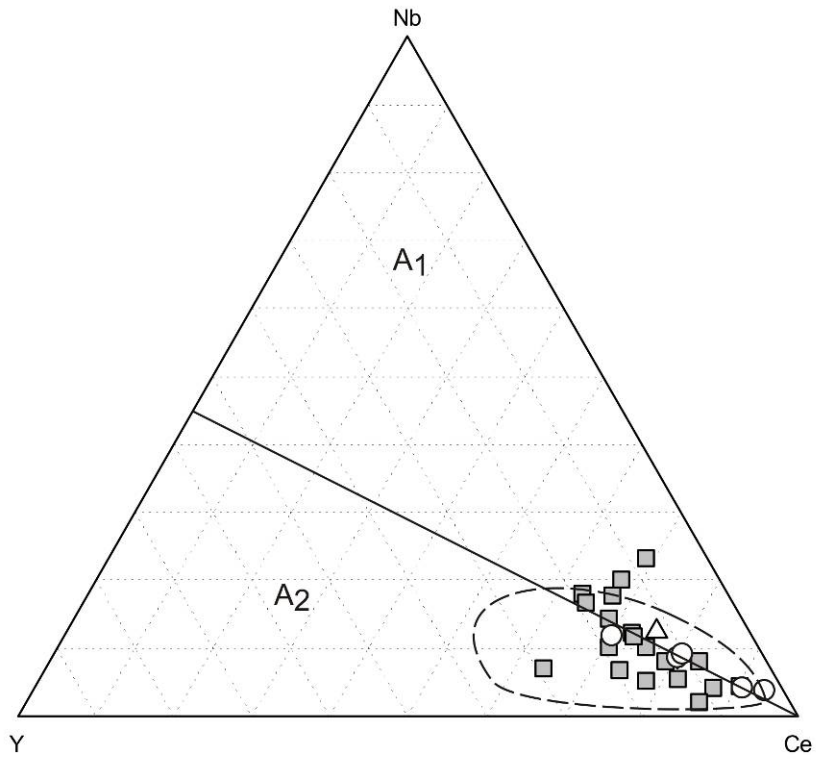
971
972 Fig. 8 a)



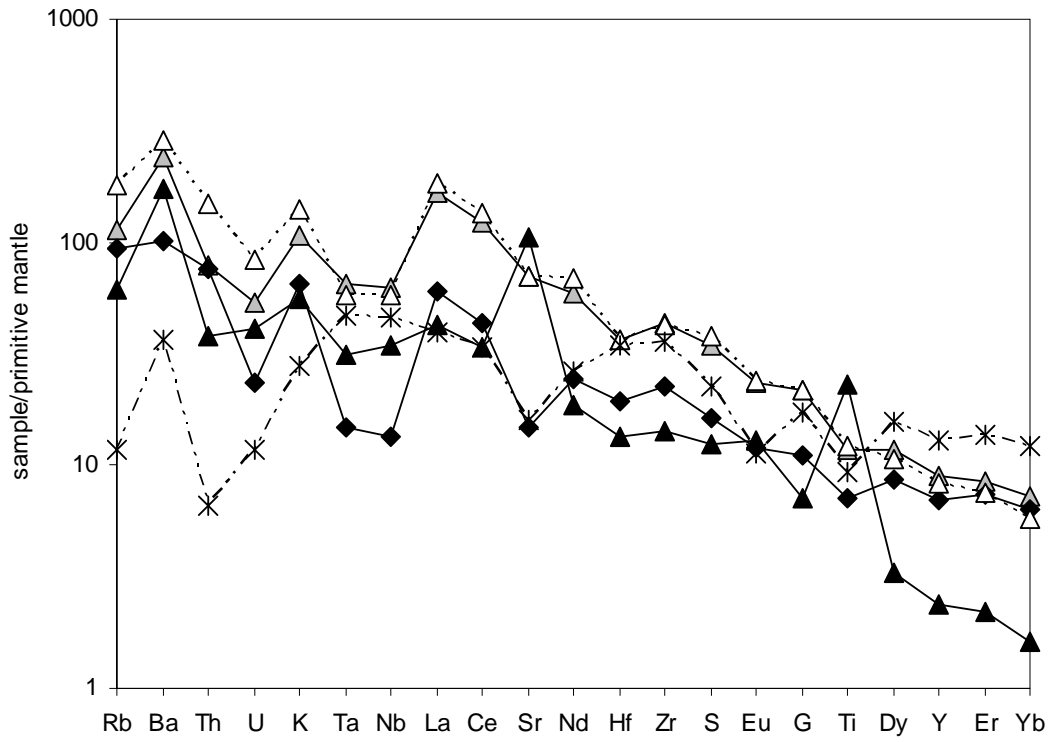
973
974 Fig. 8 b)



975
976 Fig. 8 c)

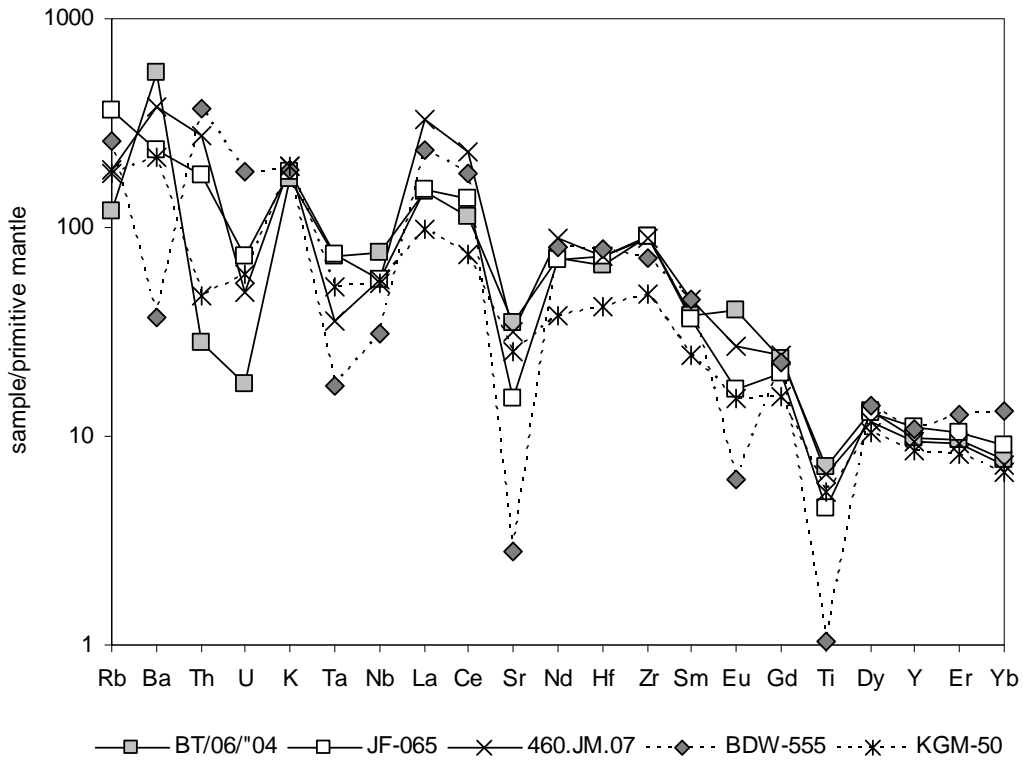


977
978 Fig. 8 d)

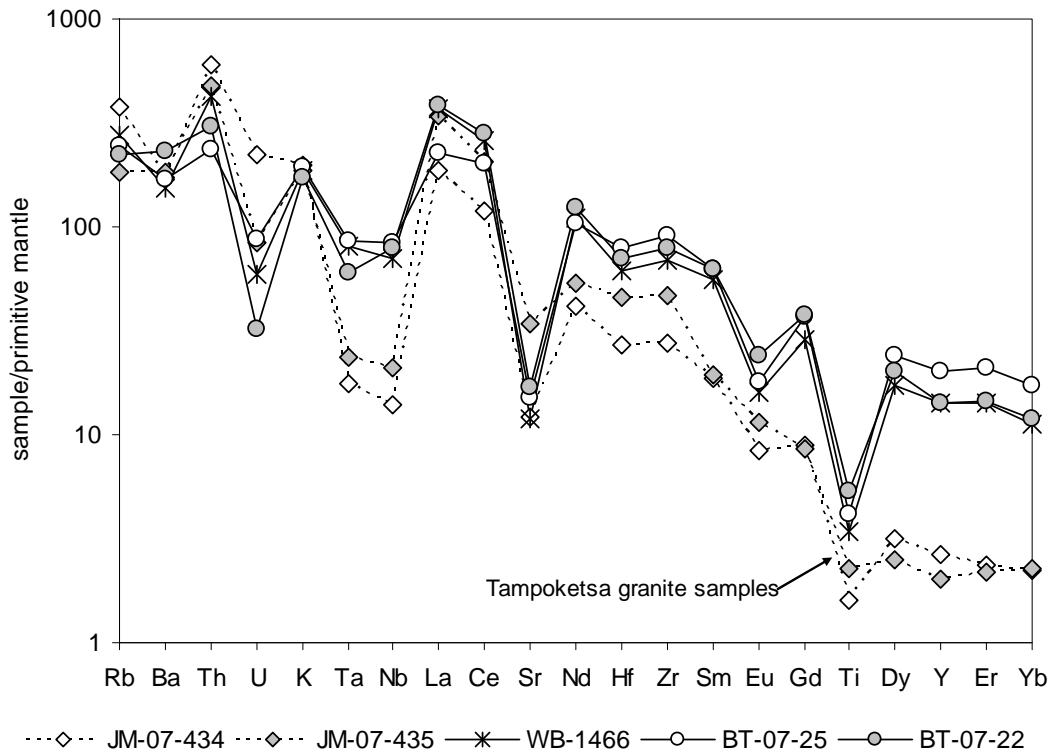


—△— WB-1471 —◆— RT-06-465 ...△... BT-07-12 —▲— 497.JM.07 --*-- KGM-48

979
980 9 a)



981
982 9 b)



983
984 9 c)